KTH ROYAL INSTITUTE
OF TECHNOLOGY

Doctoral Thesis in Fibre and Polymer Science

Lignin-Based Thermosets with Tunable Mechanical and Morphological Properties

A Study of Structure-Property Relationships

IULIANA RIBCA

Stockholm, Sweden 2023

Lignin-Based Thermosets with Tunable Mechanical and Morphological Properties

A Study of Structure-Property Relationships

IULIANA RIBCA

Academic Dissertation which, with due permission of the KTH Royal Institute of Technology, is submitted for public defence for the Degree of Doctor of Philosophy on Thursday the 15th June 2023, at 10:00 a.m. in F3, Lindstedtsvägen 26, Stockholm

Doctoral Thesis in Fibre and Polymer Science
KTH Royal Institute of Technology
Stockholm, Sweden 2023

ISBN 978-91-8040-567-6
TRITA-CBH-FOU-2023:19

Printed by: Universitetsservice US-AB, Sweden 2023

To my mother and grandfather,

Mamei şi *bunelului meu*

Mama - cea care mi-a dăruit aripi

Bunelu - cel care m-a învăţat să zbor

Abstract

Nowadays, there is an urgent need to decrease our dependence on fossil resources and shift towards the use of renewable resources for advancing sustainable development. Utilizing renewable and bio-based raw materials, such as lignocellulosic biomass, for designing new materials is a promising approach to promote this objective. The main components of lignocellulosic biomass are cellulose, hemicellulose, and lignin. Lignin is the most abundant aromatic biopolymer in nature and it is produced on a large scale from chemical pulping processes as technical lignin. Lignin has the potential as a sustainable and renewable alternative to fossil-based aromatics in various applications, e.g. thermosetting resins.

Technical lignin has a complex and heterogeneous structure, with a relatively low chemical reactivity. It is characterized by a high dispersity, the presence of various functional groups that are unevenly distributed along the lignin chains, and various interunit linkages between the monoaromatics. To overcome the challenges associated with lignin heterogeneity, technical lignin can be fractionated and/or chemically modified.

In this work, LignoBoost Kraft lignin was used as a starting material to produce lignin-based thiol-ene thermosets. Firstly, lignin was fractionated using two approaches: 1) sequential solvent fractionation, and 2) microwave-assisted extraction. These fractionation approaches enabled access to lignin fractions with unique and tunable properties. Subsequently, lignin was chemically modified, in particular through allylation. Two allylation reagents were used: allyl chloride and diallyl carbonate. The use of allyl chloride enables a selective allylation of the phenolic OH groups, leaving the aliphatic and carboxylic acid OH groups unmodified. On the other hand, diallyl carbonate can react with all the aforementioned OH groups, leading to a higher degree of allylation. Subsequently, allylated lignin was thermally cross-linked with various polyfunctional thiols, leading to thiol-ene thermosets. The structure-property relationships of the thermosets were investigated by varying several parameters, including the lignin source, fractionation approach, chemical modification, and thiol cross-linker. By adjusting these parameters, various thermosets with tunable mechanical and morphological properties were produced. Understanding the structure-property relationships of these bio-based materials is crucial for identifying potential applications.

Sammanfattning

Nuförtiden finns det ett akut behov av att minska vårt beroende av fossila resurser och övergå till användningen av förnybara resurser och därmed avancera den hållbara utvecklingen. Att använda förnybara och biobaserade råvaror, såsom lignocellulosabiomassa, för att designa nya material är ett lovande tillvägagångssätt för att uppnå detta mål. Huvudkomponenterna i lignocellulosabiomassa är cellulosa, hemicellulosa och lignin. Lignin är naturens vanligaste aromatiska biopolymer och den produceras i stor skala från kemiska massaprocesser som tekniskt lignin. Lignin kan fungera som ett hållbart och förnybart alternativ till fossilbaserade aromater i olika tillämpningar, t.ex. g. värmehärdande hartser.

Tekniskt lignin har en komplex och heterogen struktur, med en relativt låg kemisk reaktivitet. Det kännetecknas av en hög dispersitet, närvaron av olika funktionella grupper som är ojämnt fördelade längs ligninkedjorna, och olika typer av enhetsbindningar mellan monoaromaterna. För att övervinna de utmaningar som är förknippade med ligninets heterogenitet kan lignin fraktioneras och/eller kemiskt modifieras.

I detta arbete användes LignoBoost Kraft-lignin som utgångsmaterial för att tillverka ligninbaserade tiol-en-härdplaster. Först har lignin fraktionerats med hjälp av två olika metoder: 1) sekventiell lösningsmedelsfraktionering, och 2) mikrovågsassisterad extraktion. Dessa fraktioneringsmetoder gjorde det möjligt att erhålla ligninfraktioner med unika och skräddarsydda egenskaper. Därefter modifierades ligninet kemiskt genom allylering. Två allyleringsreagens användes: allylklorid och diallylkarbonat. Användningen av allylklorid möjliggör selektiv allylering av de fenoliska OH-grupperna, samtidigt som de alifatiska och karboxylsyra-OH-grupperna lämnas omodifierade. Diallylkarbonat kan å andra sidan reagera med alla de tidigare nämnda OH-grupperna, vilket leder till en högre grad av allylering. Därefter tvärbands härdades allylerat lignin termiskt med olika polyfunktionella tioler, för att ge härdplast med tiol-en-tvärbindingar. Struktur-egenskapsförhållandena för härdplasterna undersöktes genom att variera flera parametrar, inklusive ligninkällan, fraktioneringsmetod, kemisk modifiering och tioltvärbindare. Genom att justera dessa parametrar producerades olika härdplaster med skräddarsydda mekaniska och morfologiska egenskaper. Att förstå relationerna mellan struktur och egenskaper av dessa biobaserade material är avgörande för att identifiera potentiella tillämpningar.

List of appended papers

This thesis is a summary of the following papers:

I. **Exploring the effects of different cross-linkers on lignin-based thermoset properties and morphologies**

Iuliana Ribca, Marcus E. Jawerth, Calvin J. Brett, Martin Lawoko, Matthias Schwartzkopf, Andrei Chumakov, Stephan V. Roth, Mats Johansson. *ACS Sustainable Chemistry & Engineering* (**2021**), *9* (4), 1692–1702.

II. **Effect of molecular organization on the properties of fractionated lignin-based thiol-ene thermoset materials**

Iuliana Ribca, Benedikt Sochor, Stephan V. Roth, Martin Lawoko, Michael A. R. Meier, Mats Johansson.

Under revision

III. **Impact of lignin source on the performance of thermoset resins**

Iuliana Ribca, Benedikt Sochor, Marie Betker. Stephan V. Roth, Martin Lawoko, Olena Sevastyanova, Michael A. R. Meier, Mats Johansson. *European Polymer Journal* (**2023**), 194, 112141.

IV. **Microwave-assisted fractionation and functionalization of technical lignin towards thermoset resins**

Alessio Truncali, Iuliana Ribca, Jenevieve Gocheco Yao, Minna Hakkarainen, Mats Johansson.

Manuscript in preparation

Author's contributions to the appended papers

The appended papers resulted from the collaboration with co-authors. The author's contributions are as follows:

I. Major part of the planning, experimentation, and analysis. Prepared the manuscript.

II. Major part of the planning, experimentation, and analysis. Prepared the manuscript.

III. Major part of the planning, experimentation, and analysis. Prepared the manuscript.

IV. Part of the planning, major part of experimentation, and analysis. Prepared half of the manuscript.

Scientific contributions not included in this thesis

V. Synthesis of novel polyol structures for polyurethanes and other thermosets

Experimental work (lignin epoxidation, thermoset preparation, parts of DMA, FTIR, TGA, and DSC analysis) contributing to the doctoral thesis chapter "Application of biobased aliphatic polyether and polyester diamines in thermosets". M. Rhein. *Doctoral thesis,* KIT, Karlsruhe, Germany (**2022**).

VI. Polythionourethane thermoset synthesis via activation of elemental sulfur in an efficient multicomponent reaction approach

J. Wolfs, I. Ribca, M. A. R. Meier, M. Johansson. *ACS Sustainable Chemistry & Engineering* (**2023**), *11* (9) 3952–3962.

VII. Industrial Kraft lignin based binary cathode interface layer enables enhanced stability in high efficiency organic solar cells

Qilun Zhang, Tiefeng Liu, Huotian Zhang, Iuliana Ribca, Xianjie Liu, Renee Kroon, Simone Fabiano, Feng Gao, Martin Lawoko, Mats Johansson, and Mats Fahlman.

Manuscript in preparation

Abbreviations and symbols

a.u.	Arbitrary units
AC	Allyl chloride
CO_2	Carbon dioxide
D_1	Signal associated with lignin superstructures
D_2	Signal associated with T-shaped π-π staking interactions
D_3	Signal associated with sandwiched π-π staking interactions
D_4	Signal associated with thioether organized structures
DAC	Diallyl carbonate
DMA	Dynamic mechanical analysis
DMSO	Dimethyl sulfoxide
DSC	Differential scanning calorimetry
$Đ$	Dispersity
E	Young's modulus
E'	Storage modulus
E''	Loss modulus
ene	Carbon-carbon double bond, C=C
EtOAc	Ethyl acetate
EtOH	Ethanol
FTIR	Fourier transform infrared spectroscopy
HIFP	Hexafluoro-2-propanol
HW	Hardwood LignoBoost Kraft lignin
HSQC	Heteronuclear single quantum coherence
IPA	Isopropanol
LiBr	Lithium bromide
LiOH	Lithium hydroxide
MeOH	Methanol
$MgSO_4$	Magnesium sulphate
M_n	Number-average molecular weight
M_w	Weight-average molecular weight
NaOH	Sodium hydroxide
NMR	Nuclear magnetic resonance
RT	Room temperature
RT-FTIR	Real time Fourier transform infrared spectroscopy
SDGs	Sustainable development goals

SEC	Size-exclusion chromatography
SEM	Scanning electron microscopy
SW	Softwood LignoBoost Kraft lignin
TBAB	Tetrabutylammonium bromide
T_g	Glass transition temperature
TGA	Thermogravimetric analysis
THF	Tetrahydrofuran
WAXS	Wide angle X-ray scattering
ε_b	Elongation at break
σ_b	Stress at break
3TMP	Trimethylolpropane tris(3-mercaptopropionate)
4PER	Pentaerythritol tetrakis(3-mercaptopropionate)
6DPER	Dipentaerythritol hexakis-(3-mercaptopropionate)

Table of contents

1 Introduction

1.1 Sustainable materials

In 2015, the United Nations adopted 17 sustainable development goals (SDGs) as part of "The 2030 Agenda for Sustainable Development". The SDGs are interconnected and aim to address the social, economic, and environmental challenges facing the world today.[1] Sustainable development refers to the "development that meets the needs of the present without compromising the ability of future generations to meet their own needs."[2] In order to achieve this, the use of nonrenewable finite fossil-based resources should be avoided. Also, the produced materials must have a reduced environmental impact, which involves minimizing their carbon footprint (the mass of CO_2 released into the atmosphere per unit mass of produced material) and embodied energy (the energy required to produce one kg of usable material).[3,4] It is also essential to consider the circularity principles when designing new materials. The focus should be on reusability, repurposing, upcycling, and recycling when creating new materials.[5,6]

Forests are one of the largest natural resources that provide renewable raw materials. They also serve as a carbon sink by removing carbon dioxide (CO_2) from the atmosphere and storing it within the trees and soil. This process helps to mitigate climate change.[7] Forests are one of largest sources of lignocellulosic biomass, which is an excellent feedstock for sustainable energy and bio-based materials production. Lignocellulosic biomass is renewable, biodegradable, widely available, non-toxic, and generally cost-effective.[8] To achieve a sustainable development, besides the use of renewable feedstock, energy and water consumption in the production and processing processes should be minimized. The life cycle assessment of the obtained products needs to be considered as well.

In this thesis, lignin-based thermosetting materials were produced and their structure-property relationships were investigated. This research topic correlates with several SDGs, particularly SDG 12, 13, 14, and 15. These SDGs aim to promote the use of renewable resources for materials design, thus mitigating the impact of global warming.[1] In this thesis, benign and efficient processes (initiator-free, and low temperature reactions, renewable materials, solvents with low boiling point) were studied.

The effective utilization of lignin can lead to significant advancements in achieving the SDGs and contribute to a more sustainable and circular

economy. However, in order to produce lignin-based materials that have little or no negative impact on the environment, certain considerations should be considered. For example, lignin isolation should be cost-efficient and result in lignin with consistent quality. Additionally, the materials should be designed while considering the principles of circularity.

1.2 Thesis objectives and structure

The valorization of lignin into new chemicals or materials is of high interest. Lignin is the most abundant aromatic renewable resource and it is produced in large quantities, as a by-product, from pulp and paper industries. Besides its great potential in replacing fossil-based chemicals, the use of lignin is challenging due to its complex chemical structure and heterogeneity.[9,10] Lignin's native structure is impossible to preserve during the extraction conditions.

In this thesis, fractionation, chemical modification, and thermally induced cross-linking reactions of technical lignin were investigated. The main objective was to produce lignin-based thermosets with tunable mechanical and morphological properties. An extensive study to understand how the structure-property relationships affects the properties of the thermosets was conducted.

This thesis summarizes different lignin fractionation approaches, such as sequential solvent fractionation and microwave-extraction. Two different allylation reactions were investigated to give selectively allylated lignin and highly functionalized lignin fractions. Lignin-based thiol-ene thermosetting resins, with tunable properties, were produced.

A schematic overview of the work presented in this thesis is shown in Figure 1. In all papers, lignin fractionation, chemical modification, and thermal cross-linking were discussed. In *Paper I*, the effect of different polyfunctional thiol cross-linkers was investigated while keeping the lignin component constant. Technical lignin was selectively allylated with allyl chloride. In *Papers II* and *III,* the role of the lignin source was studied. Softwood and hardwood technical lignins were sequentially solvent fractionated and functionalized using diallyl carbonate. In *Paper IV,* the role of the extraction procedure on the thermosets' properties was elucidated. Various lignin fractions were extracted and chemically modified using a microwave-assisted process.

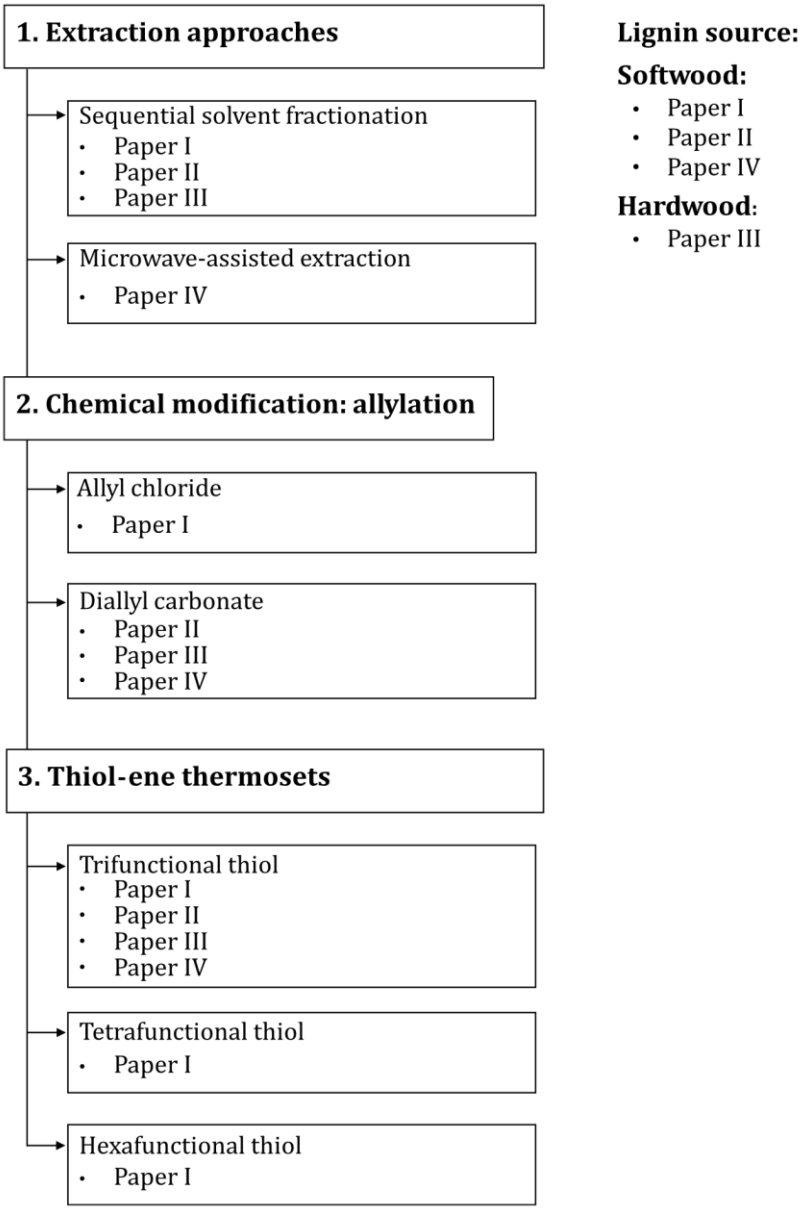

Figure 1. Schematic overview of the work presented in this thesis. In all studies LignoBoost Kraft lignin was used.

2 Background

2.1 Lignin structure

Wood is a natural composite material, mainly composed of cellulose, hemicellulose, and lignin. Lignin is an aromatic biopolymer that has multiple roles in plants, including structural function (giving rigidity and hardness to plant tissue), biological function (forms a defensive barrier against insects and fungi attacks), and water transport through the vascular tissues.[11] Lignin is a heterogeneous biopolymer, with a three-dimensionally branched architecture and a complex chemical structure.

The main building blocks of lignin are the hydroxy-cinnamyl alcohols: *p*-coumaryl alcohol, coniferyl alcohol, and sinapyl alcohol (Figure 2).[12,13] These monolignols vary by the number of methoxy substituents on the aromatic rings. Coniferyl alcohol contains one methoxy group, sinapyl alcohol contains two methoxy groups, and *p*-coumaryl alcohol does not contain any methoxy groups.[14] These variations in monolignol structure influence the chemical structure of lignin and its properties. When incorporated into the lignin's backbone, the three monolignols generate the H (*p*-hydroxyphenyl), G (guaiacyl), and S (syringyl) units (Figure 2).[15-17]

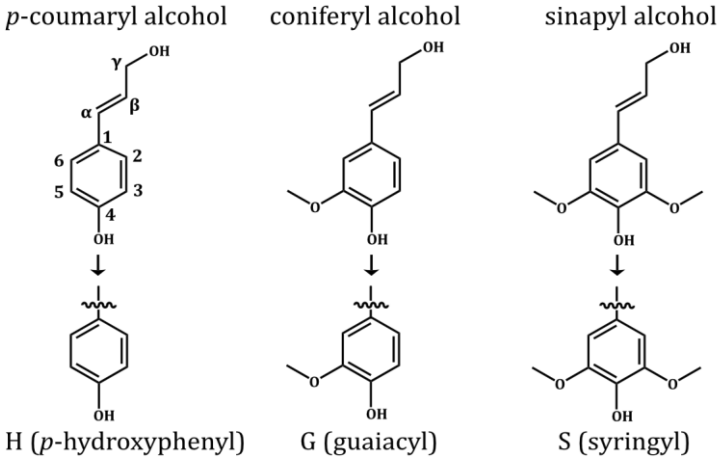

Figure 2. Lignin main building blocks (with the numbering system) and the phenylpropanoid units. Adapted from ref. 13.

The amount of G, S, and H units in lignin can vary significantly depending on the plant source. The dicotyledonous angiosperm (hardwood) lignin is mainly composed of S and G units, with small amounts of H units. The gymnosperm (softwood) lignin is mostly composed of G units, with small amounts of H units. Lignin present in grasses (monocots) has comparable amounts of G and S units and a relatively higher content of H units.[18] These units are randomly connected through C-O or C-C linkages, such as β-O-4', β-5', β-1', β-β', 4-O-5', or 5-5' (Figure 3).[15,19-21] The β-O-4' linkage is most abundant linkage within the native lignin's backbone and is relatively labile. The lignin interunit linkages can be studied by 2D NMR (nuclear magnetic resonance), and particularly HSQC (heteronuclear single quantum coherence).[9]

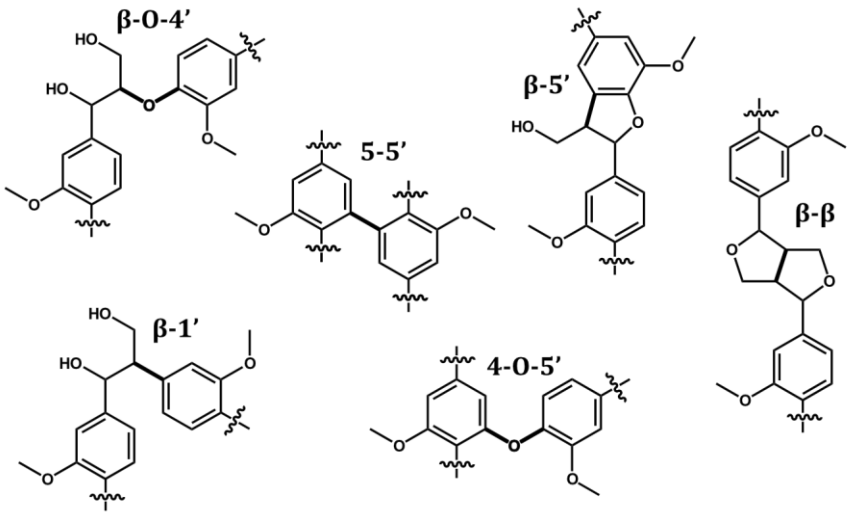

Figure 3. Interunit linkages present within softwood lignin. Adapted from ref. 13,22.

Lignin has various functional groups, such as hydroxyl, benzyl alcohol, carbonyl, and methoxy groups. The amount of hydroxyl functional groups affects lignin's reactivity towards different chemical reactions during its biosynthesis. These groups can consist of phenolic OH (syringyl, guaiacyl, *p*-hydroxyphenyl, or C_5-substituted), aliphatic OH, or carboxylic acid OH groups

(Figure 4). These groups can be identified and quantified with ^{31}P NMR following derivatization with an phosphorus reagent.[23,24]

Various analytical techniques can be used to elucidate the molecular structure of lignin and its chemical properties.[25-27] Nevertheless, lignin's heterogeneity makes its characterization challenging. It is of high interest to improve the accuracy of the developed analytical methodologies to characterize lignin qualitatively and quantitatively. The exact structure of native lignin is still under investigation and remains a topic of high debate in the scientific community.

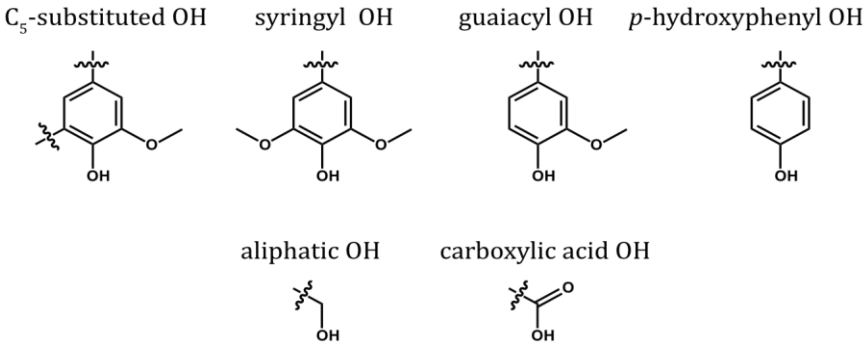

Figure 4. Various hydroxyl (OH) groups present within lignin backbone. Adapted from ref. 23.

The chemical structure of lignin enables the formation of multiple inter- and intramolecular interactions e.g. hydrogen bonds, CH-π bonds, and π-π stacking interactions. The β-O-4' can generate folded structures, facilitating the formation of the π-π stacking interactions.[28] These interactions influence lignin's properties e.g. solubility/miscibility with a variety of solvents, its self-assembly, superstructure formation, and morphology.[9,29,30]

Understanding the relationships between the lignin structure, noncovalent interactions, and the resulting properties is essential for improving lignin extraction processes and its valorization.

2.2 Isolation of technical lignin

Lignin extraction is the first step to be performed before its valorization, modification, or incorporation into materials. Lignin isolation from lignocellulosic biomass is highly challenging, due to the complex chemical interactions that occur between lignin and the other components, such as hemicellulose and cellulose. Lignin is produced on a large-scale by the pulp and paper industries, as a byproduct of pulp production.[9] The most common methods for lignin isolation can be classified into two groups; sulfur-bearing processes (Kraft pulping and sulfite pulping, which are the most common methods) and sulfur-free (solvent pulping and soda pulping).[15,31]

During the pulping or pretreatment processes, harsh conditions are applied, causing extensive chemical modification of lignin. This results in significant structural changes compared to the native structure. As a result, the distribution of previously mentioned interunit linkages is significantly altered, which further increases the heterogeneity and structural complexity of the extracted lignin.[32]

2.2.1 Kraft pulping and LignoBoost process

The Kraft process is dominant in the pulp and paper industries and is an important lignin supplier.[15,33] During the Kraft process, wood chips are pretreated at temperatures up to 170 °C for 2 h in white liquor, i.e. an aqueous solution of NaOH (sodium hydroxide) and Na_2S (sodium sulfide).[34] During this process, lignin is partially depolymerized into smaller fractions, that are soluble in the alkali solution. Then, the white liquor transforms into a dark brown or black mixture, called black liquor. To recover the solubilized lignin, the LignoBoost process can be used. This process mainly uses CO_2 to lower the pH of the black liquor, thus precipitating lignin.[32] At lower pH, lignin is in its protonated form. After acidification, lignin is filtered, re-dispersed, washed, and dewatered.[34,35] The LignoBoost process was implemented in Domtar's pulp mill (USA) and in StoraEnso's pulp mill (Finland).[36]

The chemical structure of the recovered technical Kraft lignin is different from that of native lignin. Certain linkages, such as aryl-ether, are more sensitive to pulping process whereas condensed structure, such as 5-5', are shown to be more resistant and may also be formed during Kraft pulping. Additionally, a significant number of new structures, such as 1-5', enol ether,

and stilbenes, are formed.[10,37] These structural differences should be considered when choosing a suitable valorization pathway.

2.3 Fractionation of technical lignins

Technical lignins are inherently heterogeneous, highly disperse, with a variety of functional groups that are unevenly distributed along the lignin chains. To address the technical challenges of lignin's heterogeneity, several fractionation processes have been developed. Lignin fractionation processes can be classified into two main approaches solvent- and membrane-mediated. [38-41] Solvent fractionation can be carried out in different ways, e.g. single-step extraction,[42-44] sequential extraction,[45,46] pH-dependent precipitation,[47,48] and fractional precipitation.[49]

Duval et. al. developed a sequential solvent fractionation method using only common industrial solvents (ethyl acetate, ethanol, methanol, and acetone).[45] This method enables to obtain homogeneous lignin fractions in terms of molecular weight and OH groups content.[39,49] Therefore, lignin fractionation can reduce the related issues to its heterogeneity, thus opening new ways of lignin valorization.

Another way to fractionate lignin is through the use of microwave-assisted extraction processes. These processes are characterized by fast heating rates and higher energy efficiency compared to traditional electrical heating.[50] This extraction can be used to obtain narrow dispersity lignin fractions using solvents with relatively low boiling points, such as ethanol or methanol.[51-53]

2.4 Chemical modification of technical lignins

The reactivity of lignin can be enhanced by modifying its chemical structure. Chemical modification can be achieved in various ways, depending on the targeted applications. Lignin's limited mechanical properties and thermal instability are limiting factors when considering its incorporation in high amounts for industrial applications.[54] The four main methods for chemical modification of lignin are: 1) depolymerization, 2) generation of new active sites, 3) modification of hydroxyl groups, and 4) production of graft copolymers.[54] From lignin depolymerization, chemicals, such as benzoquinone,[55] phenol,[56] and vanillin,[57] can be obtained. Vanillin is

produced from lignin on an industrial scale and represents a good alternative to replace the fossil-based aromatic building blocks.[58]

One way of introducing new active sites onto lignin backbone is by functionalizing the hydroxyl groups. Several reactions e.g. esterification,[59] etherification,[60] or phenolation,[61] have been investigated.[54,62,63]

Reactive sites, such as allyl groups, provide new opportunities for lignin to be used in radical polymerization reactions. Allylation can be achieved in various ways using allyl chloride,[64] allyl bromide[65], diallyl carbonate,[66] acryloyl chloride,[67] methacryloyl chloride,[68] allyl alcohol,[69] vinyl ethylene carbonate,[70] or a two-step route using ethylene carbonate and acrylic acid.[71] Lignin can be selectively allylated, for example, at the phenolic OH groups[64] or highly functionalized, where all available OH groups can be fully or partially allylated.[66] Allylated lignin can be used to produce thermosetting resins through thiol-ene chemistry.[64,72]

2.5 Thermosetting resins

Polymers can be classified into two categories; thermoplastics and thermosets. Thermosets are a type of polymeric material that form an irreversible chemical network through covalent cross-linking. These materials once cured cannot flow, be dissolved, be molded or melted with the same range of temperature. The curing process can be initiated through the application of heat or by addition of a chemical initiator. Thermosets have a strong and rigid 3D structure.[73,74] The properties of the thermosetting resins are mainly dependent on the chemical structure of the components, their molecular weight, and the cross-link density. Their properties can be significantly varied by simply changing the cross-link density.[75] These materials are commonly utilized in the production of epoxy adhesives and coatings, particularly in the construction and building industries. Thermosetting materials are also used for advanced applications in the aerospace and military industries.[73] Nowadays, significant research is focused on replacing the fossil-based components of thermosetting resins with bio-based alternatives.[74,76]

2.5.1 Lignin-based thermosets

Lignin's aromatic backbone and the various OH groups make it a promising substitute for fossil-based aromatic components in the development of thermosetting materials. The aromatic backbone provides stiffness, rigidity, high thermal stability, and relatively high glass transition temperature (T_g). Lignin has been utilized in the development of three main categories of thermosetting materials as reviewed recently: polyurethanes,[77] phenol-formaldehyde resins,[61] and epoxy resins.[36,78]

Previous studies have demonstrated that by combining epoxidized lignin with various amines, it is possible to produce lignin-based thermosets with tunable mechanical properties. These thermosets showed a T_g between –50 and 73 °C.[79,80]

Producing lignin-based thermosets that are mechanically and chemically recyclable is a promising approach of research that aligns with the SDGs and the transition towards a sustainable future for material production and waste management. This could be achieved by producing lignin vitrimers, which are polymeric materials with dynamic covalent bonds.[81-83] Degradable lignin-based thermosets can also be produced by cross-linking lignin with silane coupling agent.[84]

Thiol-ene thermosetting resins represent a promising class of lignin-based materials. Previously, thiol-ene thermosets were produced by using fractionated and selectively allylated lignin, with a lignin content ranging between 56 and 61 wt%. The curing reaction was thermally initiated and a trifunctional thiol cross-liker was employed. The resulting thermosets exhibited a T_g ranging from 44 to 103 °C. These thermosets had diverse nanoscale morphologies, which were corelated with the observed differences within the lignin fractions.[36] In another study, thiol-ene thermosets were produced by cross-linking the maleimide-containing lignin derivatives with various thiols. These thermosets contained between 30 and 40 wt% lignin and had a T_g ranging between –20 and 20 °C.[85]

2.5.2 Thiol-ene chemistry

The thiol-ene reaction has been known for over 100 years and involves the addition of a thiol to an ene bond.[86] These reactions can proceed under various conditions e.g. in the presence or absence of catalysts, in the presence of various solvents, at different temperatures, or in the presence of

air/oxygen/moisture (when the oxygen content is lower than the thiol content).[87,88]

The thiol-ene reaction is typically initiated either photochemically or thermally. The mechanism of this reaction proceeds with the initiation step, followed by propagation, and lastly, termination. During the initiation step, the thiyl radical is formed under irradiation with a photoinitiator or by simple thermolysis of the S-H bond. The propagation step proceeds with the addition of a thiyl radical to the ene bond, generating a carbon-centered radical intermediate. Afterwards, the chain transfer to a second molecule of thiol take place, resulting in the generation of the thiol-ene product and the simultaneous formation of a new thiyl radical. The termination step involves the coupling of two radicals to form a covalent bond. The thiol-ene reaction is a step growth polymerization.[87,89] The formed thioether bond is relatively flexible, which can result in materials with low T_g. This can limit the applications of the thiol-ene products. The T_g can be increased using rigid monomers (such as lignin), using highly functionalized cross-linkers, or by post-curing and therefore increasing the cross-link density.[90] In this thesis, allylated lignin was mixed with tri-, tetra-, and hexafunctional thiols and thermally cured. The simplified reaction mechanism of allylated lignin with a thiol cross-linker is shown in Figure 5.

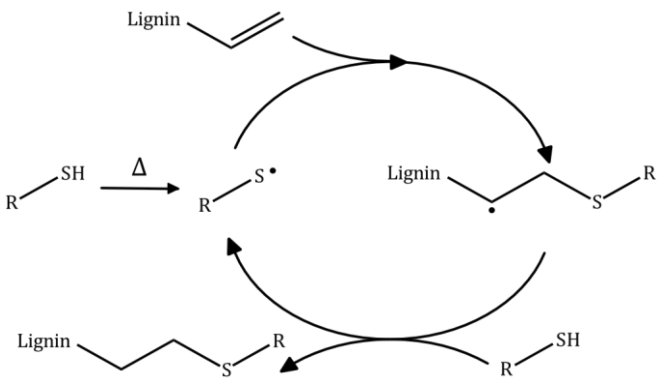

Figure 5. Simplified thiol-ene reaction mechanism of allylated lignin and thiol-cross-linker. Adapted from ref. 90.

3 Experimental

The most relevant materials used throughout this thesis and a brief description of the experimental methods and characterization techniques are reported in this chapter. Further details can be found in the appended papers.

3.1 Materials

LignoBoost Kraft Lignin: softwood lignin (SW, *Picea Abies* and *Pinus Sylvestris*) was kindly donated by Stora Enso and hardwood lignin (HW, *Eucalyptus grandis*) was extracted from kraft pulping liquor according to the LignoBoost technology.

Solvents: ethyl acetate (EtOAc, ≥99%, VWR), ethanol (EtOH, ≥99.8%, VWR), methanol (MeOH, ≥99.8%, VWR), acetone (≥99.5%, VWR), cyclohexane (99.5%, Sigma-Aldrich), isopropanol (IPA, ≥99.9%, Sigma-Aldrich).

Reagents: allyl chloride (AC, 98%, Sigma-Aldrich), diallyl carbonate (DAC, 99%, Sigma-Aldrich).

Thiol cross-linkers: trimethylolpropane tris(3-mercaptopropionate) (3TMP, ≥95%, Sigma-Aldrich), pentaerythritol tetrakis(3-mercaptopropionate) (4PER, 95%, Bruno Bock Chemische Fabrik GmbH & Co.), dipentaerythritol hexakis-(3-mercaptopropionate) (6DPER, >93%, Tokyo Chemical Industry).

Other chemicals: sodium hydroxide (NaOH, ≥98%, Sigma-Aldrich), tetrabutylammonium bromide (TBAB, 98%, Sigma-Aldrich), hydrochloric acid (HCl, 37%, VWR), magnesium sulfate ($MgSO_4$, 99%, Thermo Scientific Chemicals), lithium hydroxide (LiOH, >98%, Sigma-Aldrich). Silicone molds were prepared with a silastic T-2 base/curing agent (10:1 w/w), which were obtained from Dow Corning. All other chemicals were of analytical grade and used as received from Sigma-Aldrich.

3.2 Experimental methods

3.2.1 Lignin purification (Papers I, II, III)

The initial softwood (SW-Initial) and hardwood (HW-Initial) lignins were washed to remove impurities and to reduce the ash content. The washing step was done with 10, 20, and 35 g of lignin. Lignin samples were immersed in

deionized water and magnetically stirred for 2 h at 60 °C. The lignin to deionized water ratio was 1:20 (g/mL) in all cases. Subsequently, the lignin samples were filtered (sintered funnel, pore size 4) and the pH of the aqueous permeate was measured. This step was repeated until the pH of the aqueous permeate was above 5.5. The washed lignin samples were dried in the vacuum oven at 50 °C overnight to ensure a high dry content, which was assumed to be approximatively 95%.[91] The recovery yields were calculated to be 93 ± 2% and 80 ± 1% for SW lignin and HW lignin, respectively.

3.2.2 Sequential solvent fractionation (Papers I, II, III)

The sequential solvent fractionation approach was used in order to obtain more homogeneous lignin fractions. Four common industrial solvents, including EtOAc, EtOH, MeOH, and acetone, were employed. Roughly 15 ± 5 g of the washed lignin (softwood/hardwood) was immersed in EtOAc and magnetically stirred at room temperature for 2.0–2.5 h. The lignin to solvent ratio was 1:10 (g/mL). Afterwards, the insoluble lignin was separated by filtration from the soluble mixture using filter paper grade 3 (Munktell). The EtOAc soluble lignin fraction was subsequently rotary evaporated and both the EtOAc soluble and insoluble lignin were dried in the vacuum oven at 50 °C overnight. The dried EtOAc soluble fraction was redissolved in approximately 10 mL of acetone, precipitated in 200 mL of deionized water, and freeze-dried. The same extraction procedure was then applied to the recovered insoluble fraction with EtOH, MeOH, and acetone.[45]

Four soluble fractions were obtained and denoted SW/HW-EtOAc, SW/HW-EtOH, SW/HW-MeOH, and SW/HW-Acetone. After solvent fractionation, the residual lignin was denoted SW/HW-Insoluble, because it was not soluble in the four solvents used. However, SW/HW-Insoluble fractions were soluble in dimethyl sulfoxide (DMSO) and a mixture of pyridine/N-N-dimethylformamide which enabled its characterization. A schematic representation of the sequential solvent fractionation is shown in Figure 6.

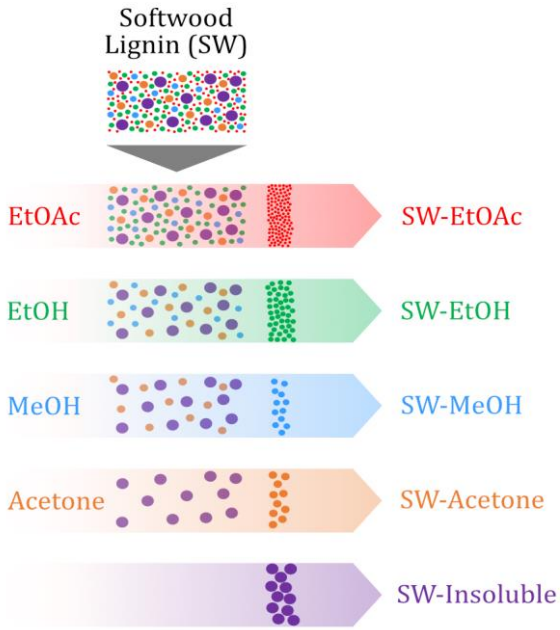

Figure 6. Simplified representation of the sequential solvent fractionation approach. Both softwood and hardwood lignin were used. In this scheme, only the softwood lignin is represented. Not to scale.

3.2.3 Microwave-assisted extraction (Paper IV)

The microwave solvent extraction approach was used to extract different lignin fractions from LignoBoost softwood Kraft lignin (SW-Initial). 2 g of softwood lignin (SW-Initial) was placed in each Teflon microwave vial (six vials in total) and 20 mL of isopropanol (IPA) was added to each vial. The closed vials were transferred to a microwave oven (model flexiWAVE, Milestone Inc.) and continuously magnetically stirred. The vials were heated to 80, 120, or 160 °C, with a ramping time of 20 min. After the samples reached the set temperature, the isotherm of 0 or 20 min was applied. Consequently, all samples were cooled to room temperature, over a period of 10 min, and left in the microwave oven for another 10 min. For some samples, pressure built up inside the vials, which was not measured or monitored. The insoluble lignin was separated by vacuum filtration. The soluble lignin was rotary-evaporated. Both soluble and insoluble lignins were dried in the

vacuum oven for 4 days at 80 °C.[51] The samples were denoted SW-IPA-temperature (°C)-isotherm (20 min)-s(soluble)/i(insoluble).

The extraction with IPA was performed by a conventional solvent extraction at room temperature (RT) for comparison. 2 g of softwood lignin (SW-Initial) were transferred to a beaker, and 20 mL of IPA was added. The mixture was magnetically stirred for 2.5 h at room temperature. Afterwards, the insoluble lignin was separated from the soluble mixture using a filter paper grade 3 (Munktell). The IPA soluble fraction was subsequently rotary evaporated and both the soluble (SW-IPA-RT-s) and insoluble (SW-IPA-RT-i) fractions were dried in the vacuum oven for at least 48 h at 80 °C. A summary of all recovered samples is presented in Table 1.

Table 1. A summary of all retrieved fractions by conventional solvent extraction and/or by microwave-assisted extraction. For each measurement, 2 g of softwood (SW) Kraft lignin were mixed with 20 mL of isopropanol (IPA). Adapted from ref. 92.

Sample name	Temperature (°C)	Isotherm (20 min)	Soluble/ insoluble
SW-IPA-RT-s	room temperature	-	s
SW-IPA-80-s	80	No	s
SW-IPA-80-I-s	80	Yes	s
SW-IPA-120-s	120	No	s
SW-IPA-120-I-s	120	Yes	s
SW-IPA-160-s	160	No	s
SW-IPA-160-I-s	160	Yes	s
SW-IPA-RT-i	room temperature	-	i
SW-IPA-80-i	80	No	i
SW-IPA-80-I-i	80	Yes	i
SW-IPA-120-i	120	No	i
SW-IPA-120-I-i	120	Yes	i
SW-IPA-160-i	160	No	i
SW-IPA-160-I-i	160	Yes	i

3.2.4 Allylation with allyl chloride (Paper I)

The SW-EtOH lignin fraction was chosen for the selective allylation toward the phenolic OH groups. 1 g of SW-EtOH lignin fraction (≈4.6 mmol of different phenolic OH groups/g lignin) was added into a two-necked round-bottom flask containing 55 mL of EtOH/NaOH (60:40, v/v) solution, which contained 1.4 mmol of NaOH. The mixture was magnetically stirred at 65 °C under reflux in an oil bath, until all lignin was dissolved. The second neck of the flask was sealed with a rubber septum. Then, allyl chloride (AC) was added dropwise to the mixture using a syringe. Allyl chloride and NaOH were used in excess (≈1.4 mmol for 1 mmol of different phenolic OH groups). The reaction mixture was magnetically stirred for 40 h at 65 °C. Afterwards, the reaction mixture was left to cool to room temperature, 50 mL of deionized water was added, and allylated lignin was precipitated by adding 0.1 M HCl dropwise. The allylated lignin was vacuum filtrated with Munktell filter paper grade 3 and washed several times with deionized water. The recovered lignin was redissolved in 15 mL of acetone, precipitated in 200 mL of deionized water, freeze-dried, and dried in the vacuum oven for at least 24 h at 50 °C.[64,91,93] The obtained powder was denoted AC-SW-EtOH. A simplified representation of the allylation reaction with AC is shown in Figure 7.

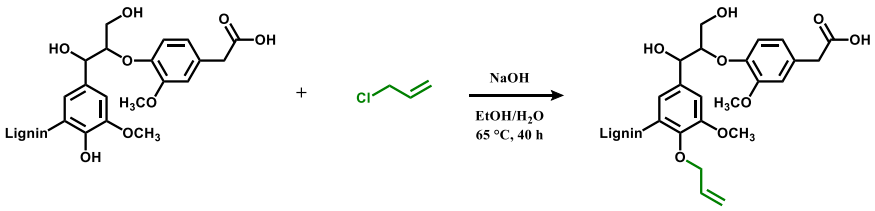

Figure 7. Simplified representation of selective SW-EtOH allylation with allyl chloride, assuming that all phenolic OH were functionalized. Adapted from ref. 91.

3.2.5 Allylation with diallyl carbonate (Papers II and III)

The initial softwood and hardwood technical lignins, as well as all lignin fractions (obtained by sequential solvent fractionation approach), were highly functionalized using diallyl carbonate (DAC). 1 g of each of the different lignin samples (≈6.5 mmol of various OH groups/g lignin) was placed in 10

mL pressure vials. Roughly 2.8 g of DAC (3 eq/lignin OH groups) and ≈2.1 g of tetrabutylammonium bromide (TBAB, 1 eq/lignin OH groups) were added to the pressure vials. The vials were sealed and magnetically stirred at 120 °C for 5 h. Subsequently, the reaction mixtures were left to cool to room temperature, dissolved in EtOAc and transferred into separatory funnels. TBAB was recovered using liquid/liquid extraction (EtOAc/deionized water). The deionized water was rotary-evaporated and the recovered TBAB (calculated yields ≥85%.) was dried in the vacuum oven at 50 °C overnight. The organic phase was dried over $MgSO_4$, filtered, concentrated to 5 mL using rotary-evaporation, and precipitated in 200 mL cold cyclohexane. The obtained allylated lignin was vacuum filtered with a Munktell filter paper grade 3, washed several times with cyclohexane, and dried in the vacuum oven for at least 24 h at 50 °C.[66,94,95] The obtained allylated lignin samples were denoted DAC-SW/HW-Initial, DAC-SW/HW-Solvent (Solvent = EtOAc, EtOH, MeOH, Acetone), and DAC-SW/HW-Insoluble. A simplified representation of the allylation reaction with DAC is shown in Figure 8.

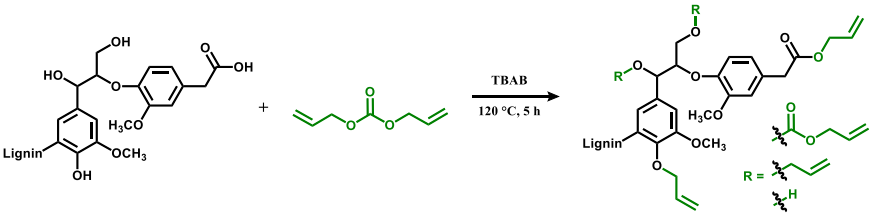

Figure 8. Simplified representation of SW and HW lignin functionalization with diallyl carbonate, assuming that all phenolic and carboxylic acid OH groups were functionalized. Reprinted from ref. 95.

The allylation reaction with DAC was performed also on SW-IPA-120-I-s samples in a microwave oven (model flexiWAVE, Milestone Inc.). Exactly the same amounts of reagents were used. Lignin sample, together with DAC and TBAB were placed in Teflon microwave vial and thoroughly mixed. The vial was closed and transferred to the microwave oven and continuously magnetically stirred. Afterwards, the vial was heated to 110 °C, with a ramping time of 5 min. After the sample reached the set temperature, the isotherm of 15 min was applied. Consequently, the sample was cooled to room temperature, over a period of 10 min, and left in the fume hood for

another 10 min. Some observable pressure built up inside the vials which was not measured or monitored. The lignin was recovered in the same way as mentioned previously. The allylated sample was denoted DAC-SW-IPA-120-I-s.

3.2.6 Decarboxylation of allylated lignin (Papers II and III)

The decarboxylation reaction was performed to determine which chemical reaction (etherification, carboxyallylation, or esterification) took place at the different OH groups present on the technical lignin backbone. This reaction was done on DAC-SW/HW-Lignin (allylated samples obtained from initial softwood and hardwood lignin and on their retrieved fractions by sequential solvent fractionation). 0.1 g of SW and HW lignin (≈6.5 mmol of different OH groups/g lignin) were dissolved in 1 mL of tetrahydrofuran (THF). For 1 mmol of the different OH, approximatively 100 mg of LiOH was added, which was firstly dissolved in 1 mL of deionized water. The reaction mixture was magnetically stirred at room temperature for one week. Afterwards, the decarboxylated lignin was precipitated by adding 1 M HCl (≈100 mL), filtered, and washed with extra HCl and deionized water. The recovered lignin was dried in the vacuum oven at 50 °C overnight.[66,95] The obtained samples were denoted D-DAC-SW/HW-Initial, D-DAC-SW/HW-Solvent (solvent = EtOAc, EtOH, MeOH, Acetone), and D-DAC-SW/HW-Insoluble. The DAC-HW-MeOH and DAC-HW-Acetone were not measured. A simplified representation of the decarboxylation reaction is shown in Figure 9.

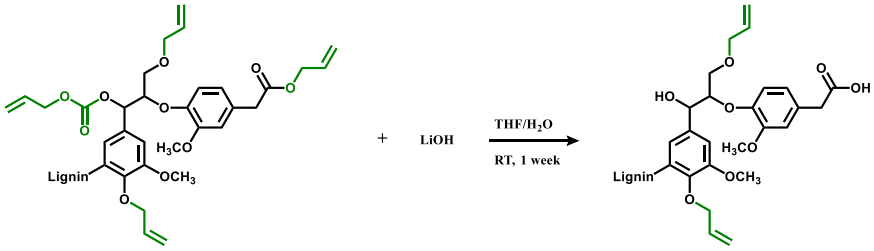

Figure 9. Simplified representation of the decarboxylation reaction of SW and HW allylated lignin, assuming that all OH groups were chemically modified were the aliphatic OH groups were partially etherified and partially carboxyallylated. Reprinted from ref. 95.

3.2.7 Preparation of thiol-ene thermosets (Papers I, II, III, and IV)

Allylated lignin samples (roughly 40 mg for each sample) were mixed with polyfunctional thiol cross-linkers (one at the time) and fully solubilized in 150 mL of EtOAc in a vial. Various thiol cross-linkers, with different numbers of functional groups per molecule (three, four and six thiol groups), were used: trimethylolpropane tris(3-mercaptopropionate) (3TMP, three SH), pentaerythritol tetrakis(3-mercaptopropionate) (4PER, four SH), and dipentaerythritol hexakis-(3-mercaptopropionate) (6DPER, six SH). The molar ratio between the reactive groups (ene:thiol) was 1:1. The mixtures were poured into silicone molds and left in the fume hood overnight to allow solvent evaporation. Afterwards, the samples were cured in the oven at 125 °C between 20–50 h. The free-standing samples were removed from the molds right after they were taken out of the oven.[64,72,91,96] The approximate dimensions of the free-standing samples were 12 mm × 5.2 mm × 0.15 mm. The obtained lignin-based thermosets were denoted: T3/T4/T6-AC-SW-EtOH, T3-DAC-SW/HW-Initial, T3-DAC-SW/HW-Solvent (Solvent = EtOAc, EtOH, MeOH, and Acetone), T3-DAC-SW/HW-Insoluble, and T3-DAC-SW-IPA-120-I-s. T3, T4, and T6 indicate if a tri-, tetra-, or hexafunctional thiol was used. A simplified representation of the thermoset's preparation is shown in Figure 10 and the thermosets composition is presented in Table 2.

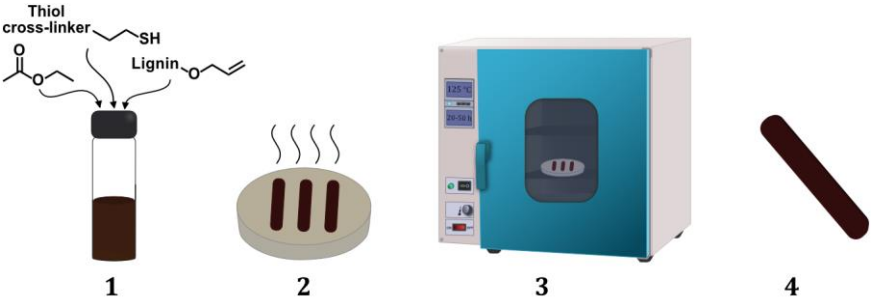

Figure 10. Allylated lignin was mixed with a thiol cross-linker and dissolved in EtOAc (1). The mixture was solvent casted (2) and cured in the oven at 125 °C (3). Free-standing lignin-based thiol thermosets were obtained (4).

Table 2. The composition of lignin-based thermosets. The standard deviation for all samples was on average ± 1%. Adapted from ref. 91, 92, 95, and 96.

	Sample name	Allylated lignin (wt %)	Thiol cross-linker (wt %)
Paper I	T3-AC-SW-EtOH	66	34
	T4-AC-SW-EtOH	68	32
	T5-AC-SW-EtOH	67	33
Paper II	T3-DAC-SW-Initial	53	47
	T3-DAC-SW-EtOAc	54	46
	T3-DAC-SW-EtOH	54	46
	T3-DAC-SW-MeOH	54	46
	T3-DAC-SW-Acetone	55	45
	T3-DAC-SW-Insoluble	58	42
Paper III	T3-DAC-HW-Initial	58	42
	T3-DAC-HW-EtOAc	56	44
	T3-DAC-HW-EtOH	58	42
	T3-DAC-HW-MeOH	57	43
	T3-DAC-HW-Acetone	60	40
	T3-DAC-HW-Insoluble	62	38
Paper IV	T3-DAC-SW-IPA-120-I-s	55	45

3.3 Characterization techniques

Additional information about sample preparation, performed measurements, and equipment details can be found in the appended papers.

3.3.1 Size-exclusion chromatography (SEC)

Size exclusion chromatography was used to determine the molecular weight (number-average M_n, and weight-average M_w molecular weight) and

dispersity (*Đ*) of the lignin samples. For softwood lignin samples the measurements were performed on a SECcurity 1260 infinity GPC System equipped with a refractive index (RI) detector, a PSS GRAM precolumn, and two PSS GRAM separation columns (particle size 10 μm and pore size 100 and 10000 Å), at 60 °C. For hardwood lignin samples the measurements were performed on a Tosoh EcoSEC HLC-8320 SEC system equipped with a three-column system: PSS PFG Micro precolumn 100, 1000 and, 10000Å). The elution solvents were DMSO/lithium bromide (LiBr) solution (for softwood lignin samples) and HFIP (hexafluoro-2-propanol)/potassium trifluoroacetate (for hardwood lignin samples). The following internal standards were used: pullulan standards with a molecular weight range of 0.342–708 kg mol^{-1} and methyl methacrylate standards with a molecular weight range of 102–981 kg mol^{-1}. The SEC data should thus be considered as trends rather than absolute values, because of the lack of calibration standards with high structural similarity to technical lignin molecules.

3.3.2 Nuclear magnetic resonance spectroscopy (NMR)

The molecular chemical structure was studied by proton (^{1}H NMR), phosphorus (^{31}P NMR), and heteronuclear single quantum coherence (HSQC NMR) nuclear magnetic resonance spectroscopy. The measurements were performed on a Bruker Avance III HD 400 MHz instrument with a BBFO probe (equipment with a Z-gradient coil). The presence of allyl functionalities was identified by ^{1}H NMR. The quantification of the different hydroxyl groups (aliphatic, phenolic, carboxylic acid), present in technical lignin, was done by ^{31}P NMR.[23] The different hydroxyl groups were phosphitylated in the presence of an internal standard and then quantified. The integration regions used for lignin were: aliphatic OH (149.5–145.5 ppm), C_5-substituted OH (144.7–140.1 ppm), guaiacyl OH (140.1–138.8 ppm), *p*-hydroxyphenyl OH (138.8–137.0 ppm), and carboxylic acid OH (136.0–133.6 ppm).[23] The allyl content was also determined by ^{31}P NMR by calculating the difference between the amount of the OH groups before and after allylation. The ^{1}H-^{13}C HSQC provided information about chemical shifts with correlation maps between directly bonded ^{1}H and ^{13}C nuclei thus enable the identification and semi-quantification of the main interunit linkages in lignin samples. The values of the interunit linkages are reported as the number of linkages per

100 aromatic units (%C_9 aromatic units) The signals of unsubstituted C_2/H_2 of the lignin aromatic groups was used as the internal standard.[37]

3.3.3 Fourier transform infrared spectroscopy (FTIR) and real time FTIR (RT-FTIR)

The chemical composition of lignin fractions and lignin-based thermosets was analyzed by FTIR. The measurements were performed on a PerkinElmer Spectrum 100 instrument equipped with a diamond crystal. The curing performance of the lignin-based thiol-ene thermosets was determined by monitoring the decrease of the absorption intensity of the thiol group signal (2607–2533 cm^{-1}) using RT-FTIR. [97]

3.3.4 Differential scanning calorimetry (DSC)

Thermal transitions of lignin samples were studied by DSC. The measurements were performed on a Mettler Toledo DSC1. The onset or midpoint of the second heating curve was taken as the glass transition temperature T_g.

3.3.5 Thermogravimetric analysis (TGA)

Thermal behavior of the lignin fractions and lignin-based thermosets was studied by TGA. The measurements were performed on a Mettler Toledo TGA/DSC1 instrument. The residual weight, as well as $T_{5\%}$, $T_{50\%}$, and T_{max} were reported, which indicate the 5%, 50%, or maximum weight loss.

3.3.6 Dynamic mechanical analysis (DMA)

The viscoelastic properties of the lignin-based thermosets in tensile mode were investigated by DMA. The measurements were performed on a DMA Q800 instrument equipped with a clamp for tensile testing. The approximate dimensions of the free-standing samples were 12 mm × 5.2 mm × 0.15 mm. Storage modulus (E'), loss modulus (E''), and *tan δ* were continuously recorded as a function of temperature. T_g of the thermosets was reported as the maximum of *tan δ*.

3.3.7 Uniaxial tensile testing

The tensile properties of the lignin-based thermosets were studied by uniaxial tensile testing. The measurements were performed on an Instron 5944 instrument equipped with a 500 N cell. The approximate dimensions of the free-standing samples were 12 mm × 5.2 mm × 0.15 mm. Young's modulus (E), elongation at break (ε_b), and stress at break (σ_b) were determined for different samples.

3.3.8 Wide angle X-ray scattering (WAXS)

Wide angle X-ray scattering measurements were performed in order to study the nanoscale morphology of the lignin fractions and lignin-based thermosets. All X-ray experiments were performed at the beamline P03 at PETRA III (Hamburg, Germany). From the intensity profiles in reciprocal space, the scattering vector q was calculated. From the peak position, of the scattering vector in reciprocal space, it was possible to calculate the so-called D-spacing ($D = 2\pi/q$). D gives information about the distances and sizes of repeating features within the analyzed samples in real-space.

4 Results and discussion

This thesis explores how to produce lignin-based thiol-ene thermosets with tunable mechanical and morphological properties. An understanding of the structure-property relationships of these thermosets is needed in order to tailor their properties for specific applications. This chapter is divided into three sections and aims to discuss the foremost results. The first section focuses on the technical lignin extraction. Two extraction approaches were evaluated: sequential solvent fractionation (Paper I, II, III) and microwave-assisted extraction (Paper IV). In the second section, lignin chemical modification was studied by employing allyl chloride (Paper I) and diallyl carbonate (Paper II, III, IV). In the last section, the lignin-based thermosets properties were discussed, focusing on the mechanical and morphological properties of the thermosets (Paper I, II, III, and IV).

4.1 Lignin fractionation

Technical lignins have a complex and heterogeneous structure, with a high dispersity and variable functional group distributions.[98] Therefore, it is difficult to characterize technical lignin and also limits its application in polymer-based materials. In order to overcome the technical lignin heterogeneity issues, different lignin fractionation approaches were developed.[40] In this thesis, two fractionation approaches were evaluated (sequential solvent fractionation[45] and microwave-assisted extraction[51]). The molecular weight, dispersity, functional groups, chemical structure, thermal behavior, and nanoscale morphology of the lignin fractions were studied.

4.1.1 Sequential solvent fractionation (Papers I, II, and III)

A sequential solvent fractionation procedure was previously developed by Duval et al. in our laboratories.[45] Four common industrially used solvents were studied: EtOAc, EtOH, MeOH, and acetone. Five lignin fractions (including the residual one) with tunable properties were retrieved. Softwood and hardwood LignoBoost Kraft lignins (which were firstly washed [91,95,96]) were used. The molecular weight distributions for the initial lignins and their fractions are shown in Figure 11. It was observed that the average

molecular weight of the soluble fractions increased from SW/HW-EtOAc to SW/HW-Insoluble. Simultaneously, the dispersity for the retrieved fractions was lower than the dispersity for the corresponding initial softwood or hardwood lignins.

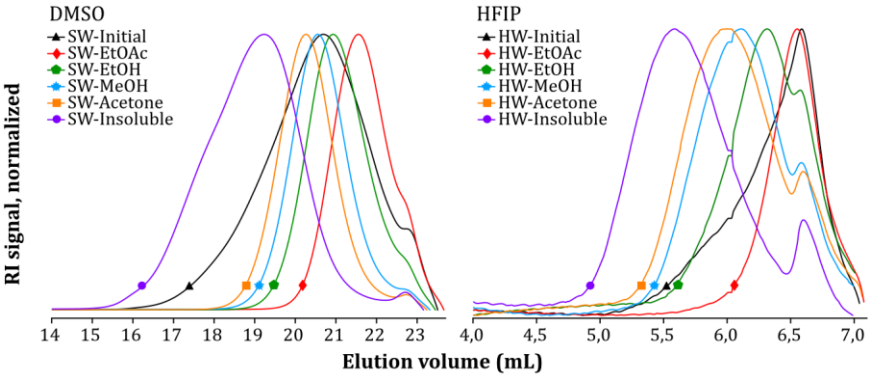

Figure 11. SEC overlay (used eluent: DMSO for softwood lignin samples and HFIP for hardwood lignin samples). Adapted from ref. 95 and 96.

The yields of the solvent fractionation approach are shown in Table 3. The solubility of hardwood lignin was higher in the chosen solvents, specifically for EtOAc and EtOH. As a result, the content of the insoluble fraction for hardwood was 14 ± 1% and for softwood it was 34 ± 1%.

Table 3. The yields (%) of the sequential solvent fractionation approach and the T_g for softwood and hardwood lignin samples are shown. Adapted from ref. 91, 95, and 96.

Sample	Yields (%)	T_g (°C)	Sample	Yields (%)	T_g (°C)
SW-Initial	–	144	HW-Initial	–	124
SW-EtOAc	23 ± 1	89	HW-EtOAc	37 ± 1	111
SW-EtOH	22 ± 1	145	HW-EtOH	28 ± 1	174
SW-MeOH	8 ± 1	181	HW-MeOH	8 ± 0	167
SW-Acetone	10 ± 1	190	HW-Acetone	7 ± 1	193
SW-Insoluble	34 ± 1	162	HW-Insoluble	14 ± 1	N/A

The thermal transition appearing in DSC thermograms was associated with the glass transition temperature. It was observed that for the SW/HW-EtOAc fractions, the T_g was lower than the corresponding initial SW or HW technical lignins. This could be due to the fact that SW/HW-EtOAc have the lowest molecular weight. The relatively high T_g, for all lignin samples, is due to the presence of hydrogen bonding, between different OH groups, and the high content of rigid aromatic rings.[46] Subsequently, lignin degradation was studied by TGA. The mass loss above 100 °C was attributed to devolatilization of moisture and residue solvents.[99] The primary mass loss was noticed between 200 and 650 °C for all fractions. The generated residue at 800 °C for softwood lignin samples was between 36–45% and for hardwood lignin samples it was between 35–41%.

The quantification of different OH groups was done by ^{31}P NMR and the results are presented in Figure 12.

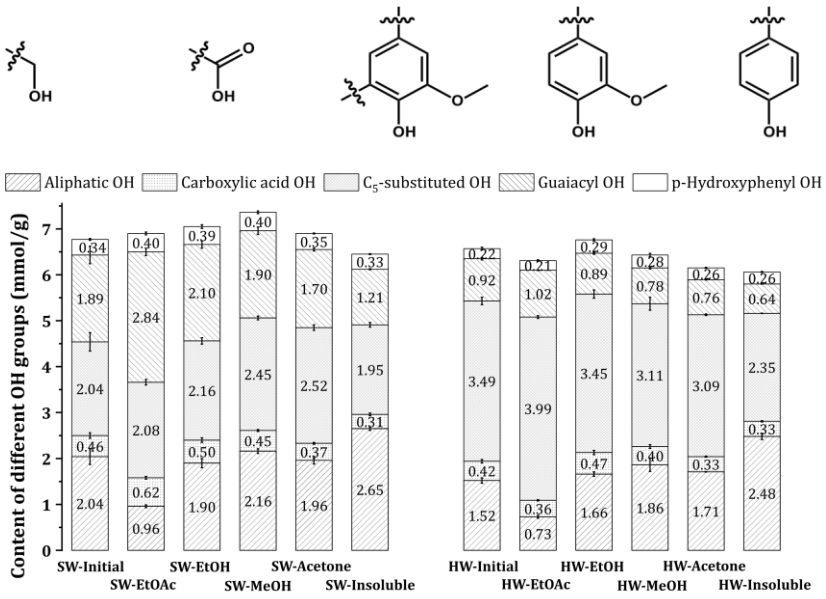

Figure 12. The quantification of different OH groups in hardwood and softwood lignin samples done by ^{31}P NMR. Data is presented in mmol of different OH groups/g of lignin. Adapted from ref. 95 and 96.

From ^{31}P NMR, it was observed that in both the softwood and hardwood retrieved fractions, the content of aliphatic OH groups increased gradually from SW/HW-EtOAc to SW/HW-Insoluble (excepting SW/HW-Acetone). The content of C_5-substituted OH was higher in hardwood lignin and the content of guaiacyl OH was relatively higher in softwood lignin. This is due to the monolignol composition of softwood and hardwood lignins. Hardwood lignin has a much higher content of syringyl units, which accounts for large part of C_5-substituted OH.[22,100] The SW/HW-EtOAc fractions have the highest content of phenolic OH groups. These fractions have the lowest molecular weight. It was shown that during the pulping process, β-O-4' linkages are cleaved and therefore more phenolic OH groups are generated.[22] Overall, softwood fractions have a slightly higher total OH groups content compared with hardwood lignin.

In addition to chemical structure and composition, the lignin morphology at nanoscale also influences its properties. Lignin can form hydrogen bonding and other noncovalent interactions, such as π-π stacking interactions. These interactions refer to the interactions between the aromatic rings containing π systems. [101,102] The π-π stacking interaction can have different geometric configurations, such as sandwiched π-π stacking interactions and T-shaped π-π stacking interaction (Figure 13).[103] These interactions play an important role in lignin self-assembly, superstructure formations, and stability of the chemical systems.[103]

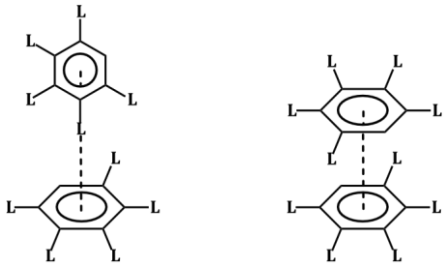

Figure 13. A schematic representation of the π-π stacking interactions present within the lignin samples. L represents the lignin backbone. Not to scale. Reprinted from ref. 95.

The presence of π-π stacking interactions within lignin samples was investigated by WAXS. In previous studies, the presence of these short

distances ordering, in the range of 4.0–4.6 Å (associated with sandwiched configuration) and 5.3–8.0 Å (associated with T-shaped configuration), was observed.[72,104,105] In this thesis, three repeating distances/sizes (D) were observed within all lignin fractions. Two signals, with lower repeating distances, were attributed to the different geometric configurations of π-π stacking interactions as following: D_2 corresponding to T-shaped π-π stacking interactions and D_3 corresponding to sandwiched (combined parallel displaced and cofacial parallel stacked).[72,91,95,96]

The D_1 signal, with the sizes/distances between 7.9–12.8 Å, was attributed to the lignin superstructures, which can be intra- or intermolecular.[95] These values are related to the maximum of the D_1 signal. All the data related to the repeating sizes/distances are shown in Table 4.

Table 4. The distances (Å) and the content (%) of the repeating features within SW/HW-Lignin samples determined by WAXS. The standard deviation for all samples was <0.15 Å. For D_1, D_2, and D_3 signals, the displayed values (in Å) represent the maximum of their signal. The content (%) was calculated by dividing the area of each signal by the total area (the sum of D_1, D_2, and D_3) and multiplied by 100. Adapted from ref. 95 and 96.

Sample	D_1 (Å)	Content (%)	D_2 (Å)	Content (%)	D_3 (Å)	Content (%)
SW-Initial	10.47	3	5.88	22	4.09	75
SW-EtOAc	7.85	7	5.52	15	4.13	79
SW-EtOH	10.70	6	5.95	17	4.18	77
SW-MeOH	10.33	8	5.94	11	4.25	81
SW-Acetone	11.01	8	5.99	13	4.27	79
SW-Insoluble	10.47	4	6.36	9	4.37	87
HW-Initial	10.47	4	6.66	19	4.14	77
HW-EtOAc	10.47	5	6.52	15	4.16	80
HW-EtOH	10.47	8	6.75	12	4.25	79
HW-MeOH	10.47	6	6.87	14	4.24	80
HW-Acetone	12.82	2	6.91	22	4.08	76
HW-Insoluble	10.47	4	6.83	21	4.18	76

The sandwiched π-π stacking interactions are the dominant ones within all lignin fractions and account for 75–87% of the interactions in softwood lignin and between 76–80% in hardwood lignin. The content of T-shaped π-π stacking interactions was between 9 and 22% for softwood samples and between 12 and 22% for hardwood samples. The distances for T-shaped π-π stacking interactions varied between softwood and hardwood lignins. In softwood lignin, the distances for the T-shaped π-π stacking interactions were between 5.5–6.4 Å, while in hardwood the distances for the same interactions were between 6.5–6.8 Å. This indicates that hardwood lignin has a more open structure. It can be related to the steric hindrance of the methoxy groups, which is higher in hardwood lignin (higher syringyl content). At the same time, the more open structure can be related to the different side chains or linkages present within the lignin backbone.

These results showed that a wide variety of starting materials can be retrieved from technical lignin. The obtained fractions differ in terms of molecular weight, dispersity, OH group distribution, and their nanoscale morphologies. Furthermore, the reactivity of these fractions can be enhanced by chemically modifying the OH groups, thus enabling their use as starting material for resin synthesis.

The solubility of lignin fractions, in various solvents, depends on a combination of multiple factors including molecular weight, monolignols distribution, functional group content, interunit linkages, and morphology

4.1.2 Microwave-assisted extraction (Paper IV)

Microwave-assisted extraction with isopropanol process was used to fractionate softwood technical lignin under mild, non-catalytic conditions. Utilizing microwave conditions can accelerate chemical reactions, leading to shorter reaction time and higher energy efficiency.[106] Six soluble and six insoluble lignin fractions were obtained by microwave-assisted extraction. For comparison, the extraction with isopropanol at room temperature was also performed.

The molecular weight distribution of the retrieved fractions and the initial lignin are shown in Figure 14. It was observed that the molecular weight and Đ for the soluble fractions were lower compared to the insoluble fractions and the initial lignin. This indicates that only the low molecular weight fractions are soluble in isopropanol during the microwave processing. It is

not clear whether these low molecular fractions were already present in the technical lignin or were generated by possible partial lignin depolymerization.[107] All soluble samples showed similar molecular weight and Đ, with no significant differences. In contrast, the molecular weight and Đ of the insoluble fractions were significantly higher. It was also noticed that the molecular weight of the insoluble fractions increased when increasing the temperature and reaction time. This increase in molecular weight could be attributed to lignin repolymerization.[107]

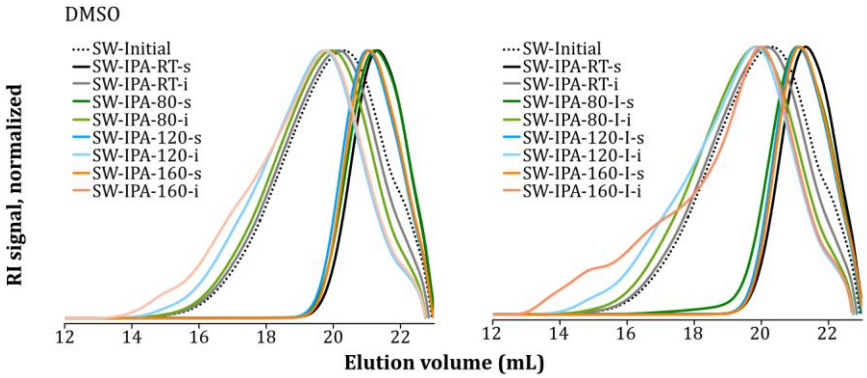

Figure 14. SEC overlay (used eluent: DMSO) for microwave-assisted extracted lignin fractions. Adapted from ref. 92.

The yields of the extraction processes are shown in Table 5. It was observed that the yields of the microwave-assisted extracted soluble fractions were between 2.4 and 3.3 times higher than the yield of the soluble fraction extracted with isopropanol at room temperature. The observed increase in yields could be attributed to the high temperature and pressure, which are affecting the solubility and possibly depolymerization. It was also observed that at temperatures of 120 °C, the yield slightly increased (from 21 to 25%) as the extraction time increased, meanwhile no significant differences in the molecular weight and Đ were observed.

The glass transition temperature was reported in Table 5. It was noticed that for the soluble fractions the T_g was significantly lower (which was between 64 and 79 °C) compared to the insoluble fractions (which was between 149 and 184 °C) and initial lignin (144 °C). This could be associated with the differences in molecular weight as well as functional group content,

as seen in Figure 15. Low molecular weight results in a lower content of aromatic rings, higher number of chain ends, leading to a decrease in the rigidity of the lignin chains and an increase in the free volume. Lignin thermal degradation was studied by TGA. A similar degradation behavior was noticed as for the previous samples. The generated residue at 800 °C for soluble fractions was between 22–29% and for insoluble fractions it was between 37–38%.

Table 5. Yields (%) and T_g of softwood lignin samples retrieved by microwave-assisted extraction. Adapted from ref. 92.

Sample	Yields (%)	T_g (°C)	Sample	Yields (%)	T_g (°C)
SW-IPA-RT-s	8 ± 1	64	SW-IPA-RT-i	88 ± 1	149
SW-IPA-80-s	19 ± 3	67	SW-IPA-80-i	79 ± 2	155
SW-IPA-80-I-s	20 ± 2	67	SW-IPA-80-I-i	74 ± 3	149
SW-IPA-120-s	21 ± 1	79	SW-IPA-120-i	71 ± 2	157
SW-IPA-120-I-s	25 ± 0	67	SW-IPA-120-I-i	74 ± 1	164
SW-IPA-160-s	26 ± 2	68	SW-IPA-160-i	70 ± 2	166
SW-IPA-160-I-s	24 ± 1	69	SW-IPA-160-I-i	68 ± 4	184

Functional groups are important for further chemical modification as they can act as reaction sites. The quantification of different OH groups was done by ^{31}P NMR and the results are presented in Figure 15. These data revealed that the total amount of OH groups in the retrieved fractions was similar to the amount of the OH groups in the initial lignin, but there was a significant difference in the distribution of their contents within the fractions. In the microwave-extracted soluble fractions, the aliphatic OH content was significantly lower (between 1.37 and 1.51 mmol OH/g lignin) compared with the initial lignin (2.04 mmol OH/g lignin) and insoluble fractions (between 2.47 and 2.57 mmol OH/g lignin). An inverse trend was observed for the carboxylic acid and guaiacyl OH group, where the amount was significantly higher in the soluble microwave-extracted fractions than in the insoluble fractions. The amount of C_5-substituted soluble samples was slightly higher in the insoluble fractions. Overall, the amount of phenolic OH groups was higher in the soluble microwave-extracted fractions (between

4.52 and 4.78 mmol OH/g lignin) than in the insoluble fractions (which was between 3.53 and 3.77 mmol OH/g lignin). It should also be noted that the values for the aliphatic, guaiacyl, and carboxylic OH groups of the initial Kraft lignin always lie in between the values from soluble and insoluble fractions.

The ^{31}P NMR results suggest that the solubility of the lignin samples is mainly affected by the distribution of the various OH groups, their polarity, and the lignin-solvent interactions. The lower aliphatic OH content and higher phenolic OH further support the statement that during the microwave processing, side-chain reactions and cleavage of aryl ether linkages took place.[51,92]

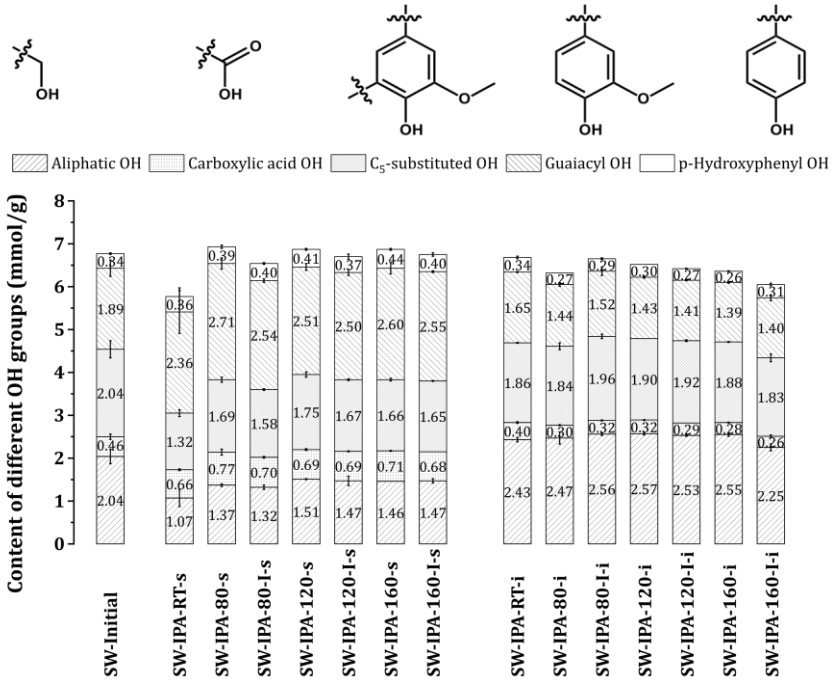

Figure 15. The quantification of different OH groups in lignin samples done by ^{31}P NMR. Data is presented in mmol of different OH groups/g of lignin.

The semiquantitative abundance of the common interunit linkages was analyzed by HSQC and the main results are shown in Table 6. It was noticed that the abundance of the β-O-4', β-5', and β-β' linkages is lower in the soluble

fractions compared to the insoluble one extracted with microwave processing. This is consistent with the ^{31}P NMR data, which suggested possible cleavage of the interunit linkages, such as aryl ether linkages, hence a higher phenolic OH content was found in the soluble fractions.

Table 6. The semiquantitative abundance (%C_9 aromatic units) of the common interunit linkages in the lignin fractions. Adapted from ref. 92.

Sample	β-O-4'	β-5'	β-β'	Stilbene β-1'	Stilbene β-5'	Enol ether
SW-Initial	6.0	2.0	1.7	4.4	10.4	2.2
SW-IPA-RT-s	3.0	1.0	0.6	9.8	6.1	1.9
SW-IPA-80-s	3.8	1.2	0.9	7.4	8.6	2.5
SW-IPA-80-I-s	4.4	1.3	0.9	9.4	9.7	3.2
SW-IPA-120-s	4.9	1.2	0.8	7.0	12.7	1.2
SW-IPA-120-I-s	4.3	1.3	0.8	8.6	7.5	2.1
SW-IPA-160-s	3.6	1.3	0.9	7.1	9.3	1.9
SW-IPA-160-I-s	3.7	1.2	0.8	7.9	9.2	2.1
SW-IPA-RT-i	9.5	3.0	2.5	4.2	11.0	3.3
SW-IPA-80-i	9.2	2.7	2.5	3.5	8.7	3.6
SW-IPA-80-I-i	9.2	2.7	2.4	3.3	6.4	3.4
SW-IPA-120-i	10.5	3.2	3.2	3.0	7.8	3.7
SW-IPA-120-I-i	9.4	2.9	3.3	4.1	8.2	3.0
SW-IPA-160-i	10.7	2.8	3.4	3.4	10.2	3.6
SW-IPA-160-I-i	7.5	3.2	3.0	2.8	11.0	2.4

4.2 Chemical modification: allylation

Technical lignin shows several limiting factors, such as heterogeneous structure and low reactivity, that restrict the design of new lignin-based materials. The introduction of chemical handles, e.g. allyl groups, provide versatile products for further utilization as thiol-ene thermoset constituents.

In this thesis, two allylation protocols were evaluated, one using allyl chloride and another using diallyl carbonate. The reaction with allyl chloride

is selective towards phenolic OH groups, meanwhile the diallyl carbonate reacts with all types of OH groups present in the lignin backbone. These OH groups, partially or completely, undergo chemical modification.

4.2.1 Allylation with allyl chloride (Paper I)

The SW-EtOH fraction was chosen for selectively allylating phenolic OH groups, due to its relatively high fractionation yield, high phenolic OH groups content, and sufficiently high molecular weight which enables minimization of monofunctional lignin chains. The allyl incorporation was confirmed by FTIR and ^{31}P NMR (Figure 16).

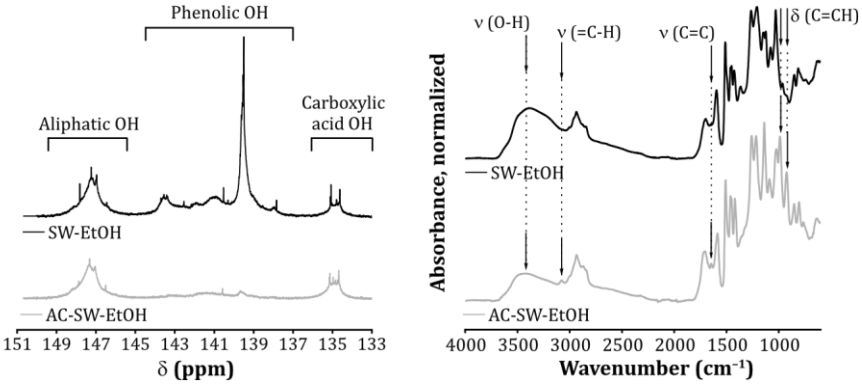

Figure 16. ^{31}P NMR (left) and FTIR (right) spectra of SW-EtOH lignin before and after allylation with allyl chloride. Adapted from ref. 91.

Four new signals were observed in the FTIR spectra, characteristic to the absorbance of the allyl groups (3077, 1647, 990, and 925 cm^{-1}). The intensity of the OH stretching vibration band decreased upon allylation, due to the consumption of free OH groups. ^{31}P NMR studies revealed that the allylation is selective towards the phenolic OH groups, with a conversion of 81 ± 4%. This also shows that the majority of the phenolic OH groups present in lignin are accessible for chemical modification, meaning that they are not "locked" within the internal lignin structure. The aliphatic and carboxylic acid OH groups were not allylated (Figure 16).

The thermal behavior of allylated lignin was investigated by DSC and TGA. A T_g of 99 °C was observed, which was lower than the T_g of the unmodified

EtOH fraction, (e.g., 145 °C). This is due to the lower hydrogen bonding capacity and introduction of more free volume generated by allyl groups. The TGA thermogram was similar to the unmodified EtOH fraction. The difference was that a more defined mass loss was observed between 200 and 315 °C. This signal could correspond to the degradation of the side chains containing allyl groups. The generated residue at 800 °C was between 41 and 45%.

4.2.2 Allylation with diallyl carbonate (Papers II, III, and IV)

Technical lignin can be highly functionalized, by targeting all OH groups, in a more sustainable approach. Diallyl carbonate was chosen as an allylating reagent. In the presence of diallyl carbonate, all OH groups will partially or completely be chemically modified. The allylation reaction with diallyl carbonate takes place fast at a relatively low temperature (120 °C). This reaction is solvent-free and it is performed in the presence of TBAB. The allylation reaction was done on the initial and sequential solvent fractionated SW/HW lignin samples (Study A, Paper II and III) and on SW-IPA-120-I-s sample (Study B, Paper IV).

Study A: allylation of solvent fractionated SW and HW samples

Initial softwood/hardwood lignins and all the retrieved lignin fractions were investigated in this study. A high functionalization of OH groups was observed by ^{31}P NMR studies (Figure 17). The phenolic and carboxylic acid OH groups were almost totally converted into allyl moieties. The phenolic OH groups underwent on average a conversion of ≥95% for both softwood and hardwood lignin samples. For the carboxylic acid OH, the average conversion was ≥85% for the softwood lignin samples and ≥91% for the hardwood lignin samples. The aliphatic OH were partially modified, with an average conversion between 43 and 75% for softwood lignin samples and 45 and 70% for the hardwood lignin samples. Overall, an average of ≥80% of the present OH groups were allylated in the softwood lignin samples and ≥77% in the hardwood lignin samples.

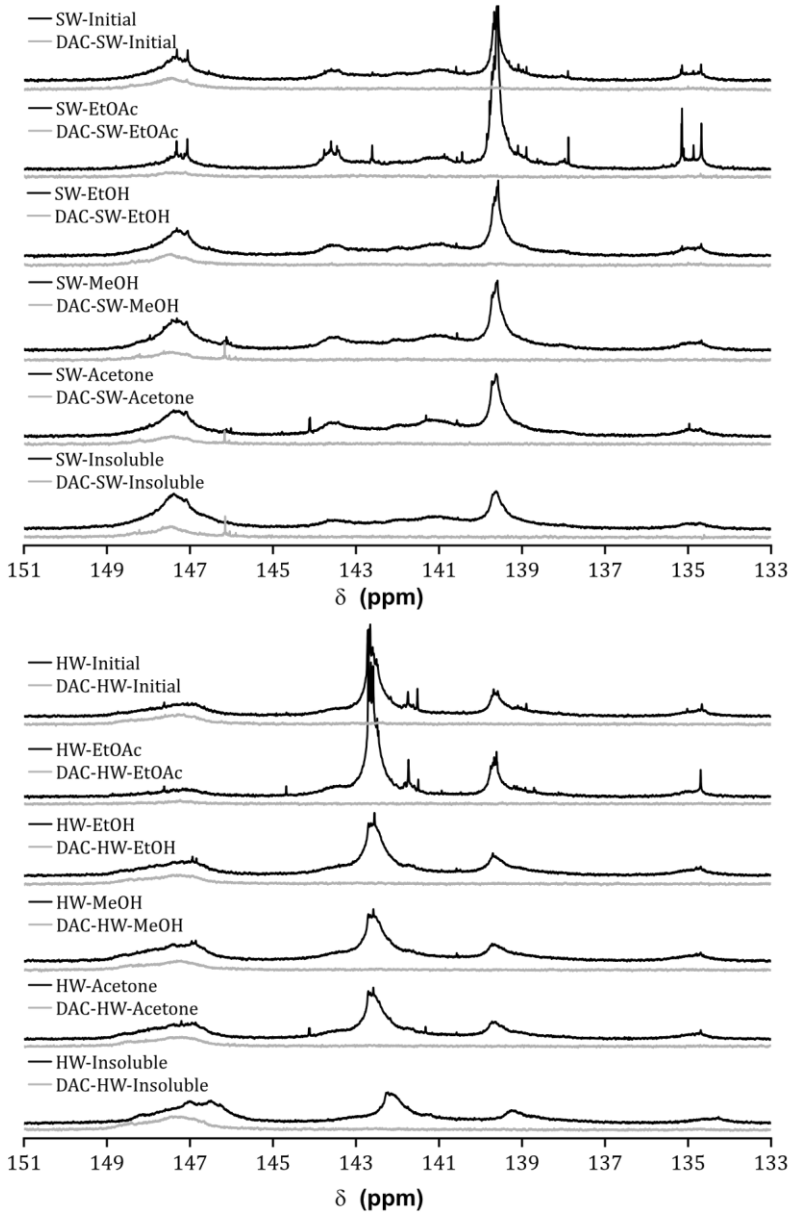

Figure 17. ^{31}P NMR spectra of SW/HW-Lignin samples before and after allylation with diallyl carbonate. Adapted from ref. 95 and 96.

In the FTIR spectra of DAC-SW/HW-Lignin samples, new signals (3077/3077, 1647/1649, 990/985, and 925/921 cm^{-1}), related to the allyl functionalities were observed. In Figure 18, only the SW/HW-EtOH and DAC-SW/HW-EtOH FTIR spectra are shown for better visualization. The intensity of the OH stretching vibration band dramatically decreased, due to the high OH groups consumption. In addition, new signals at 1743 for softwood and 1725 cm^{-1} for hardwood were observed in the allylated samples. These signals were attributed to the carbonyl C=O bond stretching, attributed to the allyl carbonates installed at the aliphatic OH groups.

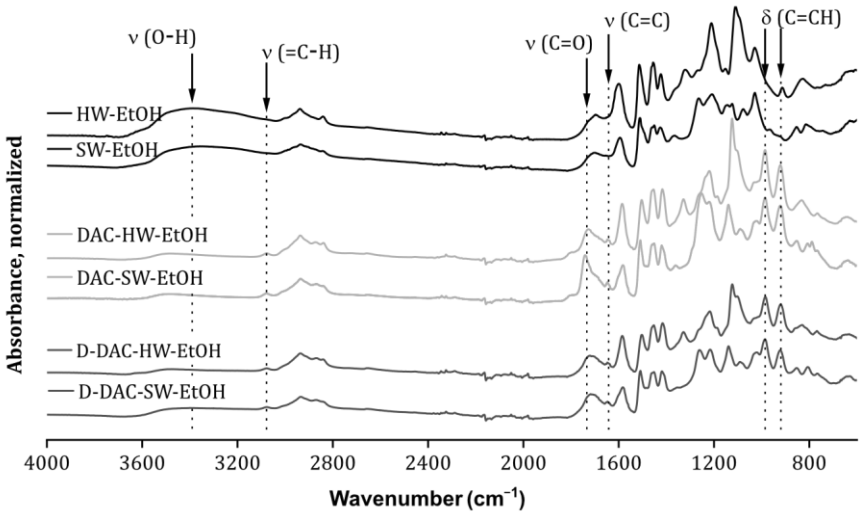

Figure 18. FTIR spectra for SW/HW-EtOH, DAC-SW/HW-EtOH, and D-DAC-SW/HW-EtOH are shown. Adapted from ref. 95 and 96.

In order to determine if the OH groups were converted into allyl esters, allyl ethers, or allyl carbonates, the decarboxylation reaction was performed on the allylated samples with DAC. In the presence of LiOH, esters and carbonates that were potentially formed will be cleaved. After the decarboxylation reaction, the carboxylic acid OH groups were fully regenerated and the amount of phenolic OH groups remained unchanged. The amount of the aliphatic OH groups decreased on average between 5 and 35% for the softwood lignin samples and between 37 and 51% for the hardwood

lignin samples. The FTIR spectra (Figure 18) of decarboxylated lignin samples showed a slight increase in the absorbance signal related to the OH stretching vibration band. The increase in this signal can be related to the partial regeneration of OH groups upon decarboxylation. Another observation was the absence of the signal at 1743/1725 cm^{-1}. ^{31}P NMR and FTIR results confirmed that the carboxylic acid OH groups were fully converted into allyl esters, the phenolic OH were fully converted into allyl ethers, and that aliphatic OH groups were partially etherified and partially carboxyallylated.

The thermal behavior of the allylated softwood and hardwood samples was investigated by DSC and TGA. The T_g of all samples was lower than the respective non-allylated fractions and it was between 32 and 93 °C for allylated softwood samples and between 61 and 112 °C for allylated hardwood samples (Table 7). This effect is mostly caused by the modification of OH groups, which further leads to a decrease of the hydrogen bonding capacity. At the same time, by introducing allyl moieties onto the lignin backbone, the free volume and molecular mobility increase. The decrease in T_g is also larger in comparison to the previous study, where only phenolic OH groups were allylated.

Table 7. The T_g of the allylated SW and HW lignin samples determined with DSC. Adapted from ref. 95 and 96.

Sample	**T_g (°C)**	**Sample**	**T_g (°C)**
DAC-SW-Initial	77	DAC-HW-Initial	89
DAC-SW-EtOAc	32	DAC-HW-EtOAc	61
DAC-SW-EtOH	71	DAC-HW-EtOH	95
DAC-SW-MeOH	83	DAC-HW-MeOH	99
DAC-SW-Acetone	93	DAC-HW-Acetone	111
DAC-SW-Insoluble	92	DAC-HW-Insoluble	112

The thermal stability of the allylated lignin samples increased, with no degradation up to 150 °C. Two distinct weight loss steps were observed. The first weight loss occurs between 150 and 300 °C for softwood lignin and between 150 and 325 °C for hardwood lignin. This weight loss was attributed to the cleavage of the propanoid side chains. The second weight loss occurs

between 300 and 600 °C for both allylated lignin types and was attributed to the rearrangement of the aromatic rings.[108] The generated residue at 800 °C for all allylated samples with DAC was between 35 and 38%.

The morphology at the nanoscale of the DAC-SW-Lignin samples was investigated by WAXS. The previously identified signals associated with lignin superstructures (D_1) and π-π stacking interactions (D_1 and D_2) were observed (Table 8). For the allylated softwood samples, the sandwiched π-π stacking interactions were still the dominant interactions, but their content decreased to 61–74%. At the same time, the content of the T-shaped π-π stacking interactions increased and was between 19 and 28%. The distances of their maximum, associated with T-shaped π-π stacking interactions, increased in allylated lignin samples by 0.54–1.33 Å. These results indicate that the allyl moieties weaken the π-π stacking interactions, consequently increasing the distances between the lignin aromatic rings, leading to a more open and accessible lignin structure. D_1, which is associated with lignin superstructures, also shifted towards larger sizes. This indicates that the allyl functionalities are situated on the "edge" of the sandwiched structures, in which the distances do not show significant change upon allylation.

Table 8. The distances and the content of the repeating features within DAC-SW-Lignin samples determined by WAXS. The standard deviation for all samples was <0.15 Å. For D_1, D_2, and D_3 signals, the displayed values (in Å) represent the maximum of their signal. The content (%) was calculated by dividing the area of each signal by the total area (the sum of D_1, D_2, and D_3) and multiplying by 100. Adapted from ref. 95.

Sample	D_1 (Å)	Content (%)	D_2 (Å)	Content (%)	D_3 (Å)	Content (%)
DAC-SW-Initial	12.63	11	7.04	28	4.11	62
DAC-SW-EtOAc	12.51	10	6.85	19	4.14	71
DAC-SW-EtOH	13.25	11	7.07	28	4.14	61
DAC-SW-MeOH	N/A					
DAC-SW-Acetone	12.80	8	6.95	25	4.17	67
DAC-SW-Insoluble	12.23	6	6.90	20	4.18	74

Study B: allylation of microwave-extracted sample

The allylation reaction conditions can be further improved using microwave heating technologies. By utilizing microwave heating, chemical reactions can be accelerated, leading to significantly reduced reaction times.[109,110] Microwave-assisted functionalization of technical lignin was performed at 120 °C in the presence of DAC and TBAB. Microwave-assisted allylation was completed after 30–40 min, which is a significant improvement in terms of energy efficiency. The OH groups were highly functionalized with allyl moieties (Figure 19). The conversion of phenolic OH groups was 96 ± 2%, of carboxylic acid OH groups was 95 ± 4%, and of aliphatic OH groups was 69 ± 9%. Overall, 90 ± 3% of the present OH groups were allylated. FTIR spectra before and upon allylation are shown in Figure 19. The four signals associated with the allyl functionalities were identified at 3077, 1643, 988, and 920 cm^{-1}. The OH groups stretching vibration band decreased after allylation. The signal at 1731 cm^{-1} attributed to the carbonyl C=O bond stretching in the allyl carbonates, installed at aliphatic OH groups, was identified in the allylated sample. The DAC-IPA-SW-120-I-s sample showed no thermal degradation up to 150 °C. The thermal degradation was similar to the previous DAC-SW-Lignin samples. The generated residue at 800 °C was 29%.

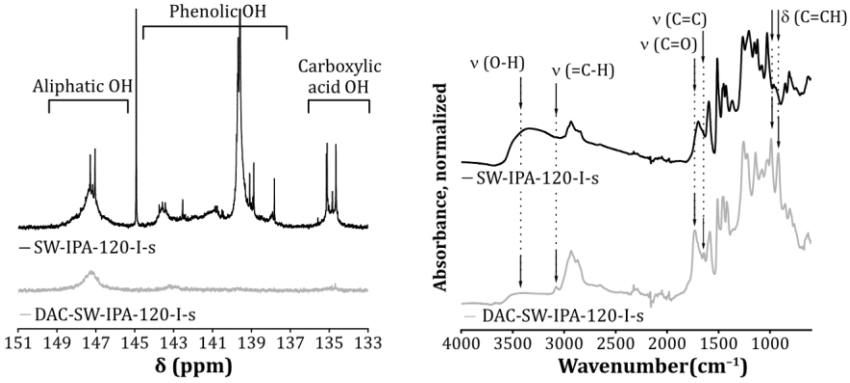

Figure 19. ^{31}P NMR (left) and FTIR (right) spectra of SW-IPA-120-I-s lignin before and after allylation with diallyl carbonate. Adapted from ref. 92.

4.3 Structure-property relationships of thiol-ene thermosets

Allylated lignin represents a promising starting material for designing thermoset materials. In this thesis, the modified lignin was mixed with different polyfunctional thiol cross-linkers, resulting in a three-dimensional network. This chapter is divided into two parts, each investigating the structure-property relationships of lignin-based thermosets. The first study elucidates the effect of different thiol cross-linkers on the properties of lignin-based thermosets. The second study was divided into two parts. In the first part, the impact of the lignin source and functionalization on the thermoset properties was investigated. The second part explored the impact of the microwave-assisted extraction procedure on the thermoset properties.

The curing temperature of 125 °C was chosen in order to further enhance the chain mobility of the allylated lignin samples (this temperature is above the T_g of allylated samples), to avoid temperatures close to lignin degradation, and prevent Claisen rearrangements, which have previously been reported to occur at temperatures above 150 °C.[65,93] The curing performance of the thermosetting resins was investigated by RT-FTIR. The consumption of thiol (2568 cm^{-1}) moieties was monitored by RT-FTIR. The curing time was set to the time when the absorption signal of thiol groups completely disappeared. The FTIR spectra, before and after curing, for all thermosetting resin formulations can be found in the appended papers.

4.3.1 The effect of different crosslinkers (Paper I)

The aim of this study was to produce lignin-based thermosets with tunable properties. In order to achieve this, the lignin part was maintained constant while the thiol cross-linker agent was varied. The AC-SW-EtOH fraction, which was selectively allylated at the phenolic OH groups with allyl chloride, was used in this study. Various polyfunctional thiol cross-linkers, with three, four, and six thiol groups per molecule, were used. The thiol:ene ratio was kept to 1:1 in all cases and the thermosets composition is reported in Table 2. The thermosets were cured for 20 h at 125 °C.

The thermoset morphology at nanoscale was studied by WAXS. The repeating distances and their content are shown in Table 9. The previous reported signals in lignin fractions, associated with different π-π stacking interactions (sandwiched and T-shaped) were observed. The sandwiched

stacking interactions are predominant and account on average for 88 ± 1%. The ratio between sandwiched and T-shaped π-π stacking interactions did not change by varying the cross-linker. The distances of the repeating features did not vary in the different thermosets. An increase in the D_2 and the D_3 signal distances was noticed compared to to the allylated lignin fraction, AC-SW-EtOH. This increase in distances indicates a more open structure. It is still not fully clear to which extent these repeating features, present within the lignin-based thermosets, influence their properties.

Table 9. The distances and the content of the repeating features within the lignin-based thermosetting samples determined by WAXS. The standard deviation for all samples was <0.10 Å. For D_2 and D_3 signals, the displayed values (in Å) represent the maximum of their signals. The content (%) was calculated by dividing the area of each signal by the total area (the sum of D_1, and D_2) and multiplying by 100. Adapted from ref. 91.

Sample	D_2 (Å)	Content (%)	D_3 (Å)	Content (%)
T3-AC-SW-EtOH	7.48	12	4.41	87
T4-AC-SW-EtOH	7.48	12	4.40	87
T6-AC-SW-EtOH	7.39	11	4.39	89

The mechanical properties of the thiol-ene thermosets were investigated by DMA. (Figure 20). The storage modulus of these thermosets at –50 °C was between 0.8 and 2.2 GPa. Moreover, when continuously increasing the temperature, the storage modulus dropped. This change in storage modulus was associated with the softening effect of the thermosets, which takes place at the glass transition temperature. The minimum values of the storage modulus were reached at temperatures between 150 and 200 °C. These minimum values provide insights into the cross-link density of the thermosets. It was noticed that the cross-link density increased with an increasing number of thiol functionalities: T3-SW-AC-EtOH < T4-SW-AC-EtOH < T6-SW-AC-EtOH.

An inverse trend was observed in the storage modulus values at temperatures below T_g. A possible explanation for this inverse trend could be related to the formation of the primary loops. In an ideal network formation process, each thiol group of a cross-linker molecule will react with a double bond from a different lignin chain. Lignin has a complex and heterogeneous

structure, thus topological defects, such as dangling chains, entanglements, and primary loops, will be generated. Primary loops are formed when a minimum of two thiol groups from the same molecule react with two double bonds from the same lignin chain, which leads to cyclization.[111] It was demonstrated that by increasing the monomer functionality in the cross-linking polymerization, a higher number of primary loops resulted as a consequence.[112] These loops consist of thioether bonds, which are more flexible compared to C-C bonds, thus leading to regions with different mobility within the thermosets network. The primary loops have a plasticizing effect and thus reduce the stiffness of the thermosets. This hypothesis is also supported by the observed morphologies at the nanoscale, where no significant differences were noticed in different thermosets. Subsequently, the thermoset stiffness below their T_g is influenced by the distribution of thioether bonds.

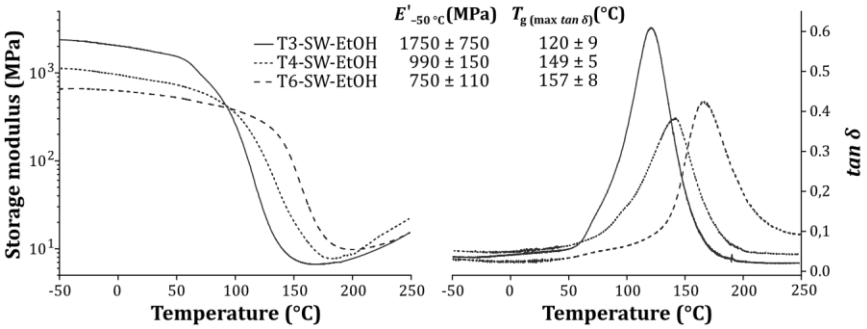

Figure 20. Representative DMA curves of the different lignin-based thermosets. Storage modulus (E') is illustrated on the left and *tan δ* on the right. Adapted from ref. 91.

The T_g of the thermosets was calculated from the maxima of the *tan δ* peak. For all thermosets, the T_g was above 100 °C, which is relatively high for a thiol-ene system. The high glass transition temperature is mainly due to the lignin chemical structure (a branched aromatic biopolymer), the cross-link density, and the noncovalent interactions (e.g., van der Waals dispersion interactions, hydrogen bonding, and π-π stacking interactions). The shape of the *tan δ* peak is related to the homogeneity of the thermoset network. The sharper and narrower the *tan δ* peak, the more homogeneous the thermoset structure is.

The T_g of the thermosetting resins increased with an increase in the number of thiol groups: T3-SW-AC-EtOH < T4-SW-AC-EtOH < T6-SW-AC-EtOH. A higher cross-link density results in a higher restriction of the chain mobility and subsequently higher T_g. The uniaxial tensile stress-stain data showed a Young's modulus (E) of 4.8 ± 1.5 GPa, a tensile stress at break (σ_b) of 68 ± 6 MPa, and an elongation at break (ε_b) of 1.5 ± 0.5%. All produced lignin-based thermosets were thermally stable up to 250 °C.

4.3.2 The impact of lignin extraction procedure, source, and functionalization (Papers II, III, and IV)

The studies presented in this chapter elucidate the impact of the extraction procedures (sequential solvent fractionation or microwave-assisted extraction), lignin source (softwood or hardwood), and high functionalization on the lignin-based thermosets' properties.

Study A: Lignin thermosets from highly functionalized softwood and hardwood lignin fractions (Papers II and III)

These studies investigate how the lignin source and its functionalization influence the thermoset properties. The allylated softwood and hardwood lignin samples and, DAC-SW/HW-Lignin, were mixed with the trifunctional thiol cross-linker. The thiol-ene ratio was kept at 1:1. The composition of the thermosets is shown in Table 2. Twelve lignin-based thermosets were obtained. The curing performance of these thermosets was investigated by RT-FTIR (Figure 21). Towards the end of the curing reaction, the thiol (2570 cm^{-1}) and ene (1642 cm^{-1}) signals disappeared, indicating that the cross-linking reaction occurred and a cross-linked network was formed.

It was noticed that all lignin resin formulations reached 95% thiol conversion after 10.6–41.2 h (Table 10). The curing reaction for the hardwood lignin resin formulations was significantly faster compared to the softwood resins. The hardwood samples reached 20% thiol conversion after 0.2–0.8 h (except T3-DAC-HW-EtOAc, 3.7 h), while the softwood samples reached the same level of conversion after 2.9–4.5 h (except T3-DAC-SW-EtOAc, 7.6 h). Hardwood samples reached 50% conversion after 0.7–2.7 (except T3-DAC-HW-EtOAc, 13.9 h) and for softwood 50% conversion was reached after 8.0–14.2 h (except T3-DAC-HW-EtOAc, 20.6 h).

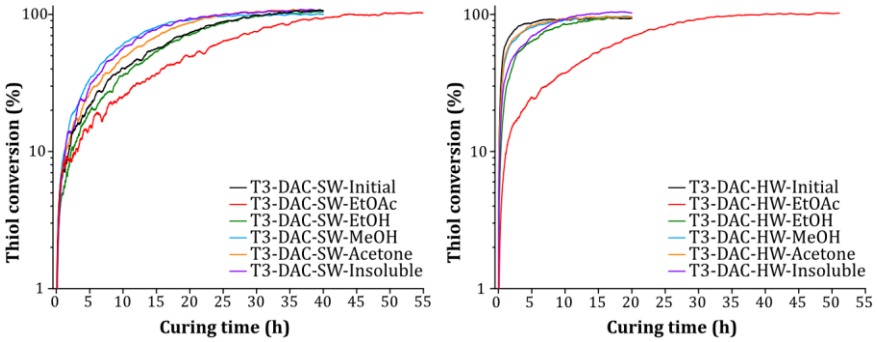

Figure 21. The thiol signal conversion (2607–2533 cm^{-1}) as a function of time for softwood and hardwood lignin resin formulations at 125 °C. Adapted from ref. 95 and 96.

In both cases, the thiol conversion for the EtOAc fraction was slower. The reason for this behavior is not clear, but it was noticed that the total content of phenolic OH groups before modification was significantly higher and the content of aliphatic OH groups was significantly lower. Subsequently, the content of aryl allyl ethers for the EtOAc samples was significantly higher compared to other samples. At the same time, the content of aryl allyl ethers was significantly lower for the T3-SW/HW-DAC-Insoluble fractions and the thiol conversion for these fractions increased faster. This suggests that the aryl allyl ethers play an important role on the curing performance of these resin formulations.

Another difference between softwood and hardwood samples is the guaiacyl content, which is significantly higher in softwood lignin. It was suggested previously, that guaiacyl structures lead to stronger intra/inter molecular interactions, making the functional groups less accessible/reactive.[30,113] The RT-FTIR results revealed that the allylated hardwood lignin samples have enhanced reactivity. This could indicate that the hardwood samples have a more open structure, therefore the allyl functionalities are more accessible. The molecular weight of hardwood lignin samples was also lower compared to softwood samples, which influences the mobility of the lignin chains and the curing performance.

Table 10. The 95% conversion of -SH signal (2607–2533 cm^{-1}), for SW/HW lignin resin formulations, during thermal curing at 125 °C. Adapted from ref. 95 and 96.

Sample	Curing time (h)	Sample	Curing time (h)
T3-DAC-SW-Initial	29.0	T3-DAC-HW-Initial	14.6
T3-DAC-SW-EtOAc	41.2	T3-DAC-HW-EtOAc	31.5
T3-DAC-SW-EtOH	29.8	T3-DAC-HW-EtOH	16.5
T3-DAC-SW-MeOH	21.8	T3-DAC-HW-MeOH	14.7
T3-DAC-SW-Acetone	23.3	T3-DAC-HW-Acetone	14.1
T3-DAC-SW-Insoluble	21.4	T3-DAC-HW-Insoluble	10.6

The morphology of the thermoset resins at nanoscale was studied by WAXS. The previously identified signals D_1, D_2, and D_3 were also present within the thermosets structure (Table 11). A new signal D_4 was identified in the lignin-based thermosets. These thermoset samples contain between 38–47 wt% thiol monomer. Therefore, this signal with distances/sizes of 3.38–3.67 Å was attributed to the thioether organized structures. A shift towards longer distances/sizes for D_1 was observed. This distance/size increase can be related to the incorporation of the thiol cross-linker and the formation of the thioether organized structures.

The signal intensity of D_1 significantly varies among different lignin-based thermosets. This indicates that the superstructure formation is affected by the film formation process. The film formation process implies physical drying (solvent evaporation) followed by a chemical cross-linking reaction, which locks the structure. Further investigation of the film formation process is needed in order to gain a better understanding of the thermoset film formation. A slight increase in the distances of D_3 signal was noticed, indicating a more open structure. The exact impact of these repeating features on the properties of the lignin-based thermosets is not fully understood.

Table 11. The distances and the content of the repeating features within T3-DAC-SW/HW-Lignin samples determined by WAXS. The standard deviation for all samples was <0.15 Å (except for T3-DAC-SW-Initial and T3-DAC-SW-MeOH, where the standard deviation for D2 was 0.5 Å). For D1, D2, D3, and D4 signals, the displayed values (in Å) represent the maximum of their signal. The content (%) was calculated by dividing the area of each signal by the total area (the sum of D1, D2, D3, and D4) and multiplied by 100. Adapted from ref 95 and 96.

Sample	D_1 (Å)	Content (%)	D_2 (Å)	Content (%)	D_3 (Å)	Content (%)	D_4 (Å)	Content (%)
T3-DAC-SW-Initial	16.17	25	6.56	23	4.35	43	3.39	8
T3-DAC-SW-EtOAc	14.62	8	6.74	21	4.42	43	3.52	28
T3-DAC-SW-EtOH	17.45	10	7.20	26	4.44	41	3.47	24
T3-DAC-SW-MeOH	14.52	10	5.51	24	4.32	52	3.41	15
T3-DAC-SW-Acetone	13.91	6	6.22	23	4.52	41	3.61	30
T3-DAC-SW-Insoluble	14.05	9	6.76	15	4.66	42	3.67	35
T3-DAC-HW-Initial	17.45	67	7.15	11	4.57	21	3.38	1
T3-DAC-HW-EtOAc	N/A							
T3-DAC-HW-EtOH	13.95	8	6.27	18	4.36	59	3.40	15
T3-DAC-HW-MeOH	14.09	8	6.12	18	4.35	59	3.41	15
T3-DAC-HW-Acetone	16.80	67	7.10	8	4.63	22	3.40	3
T3-DAC-HW-Insoluble	14.37	8	6.24	15	4.37	60	3.40	17

The mechanical properties of these lignin-based thermosets were studied by DMA and the main results are summarized in Figure 22.

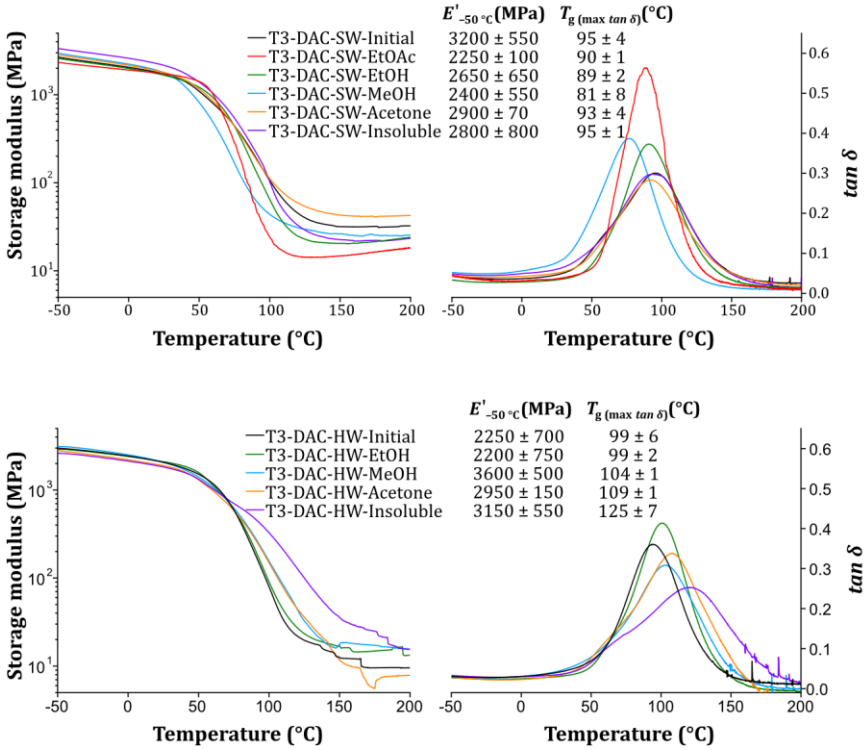

Figure 22. Representative DMA curves of softwood (top) and hardwood (bottom) lignin-based thermosets. Storage modulus (*E*') is shown to the left side and *tan δ* to the right. Adapted from ref. 95 and 96.

The mechanical properties are influenced by the cross-link density, polarity, and chain rigidity of the components. The storage modulus for all thermosets was on average between 2.3 and 3.6 GPa, which was higher compared to the previously studied thermosets, T3/T4/T6-SW-EtOH, with less functionalized lignin. Moreover, the cross-link density is higher for these thermosets, as can be seen from the storage modulus in the rubbery region. The higher storage modulus and cross-link density are due to the structural differences: the allyl content is higher, the thiol monomer content is higher,

and the polarity related to the hydroxyl groups is lower in the present study. The T_g for these thermosets was also lower compared with the previous ones. For softwood lignin-based thermosets, the T_g was on average between 89–95 °C and for hardwood lignin-based thermosets it was between 99–125 °C. The higher allyl content results in a higher content of thioether bonds. The newly formed thioether bonds are more flexible than C-C bonds, hence a low T_g is often found in thiol-ene systems.[114] This indicates that the thioether content dominates the thermosets performance. The lignin content and polarity should be considered as well. These results corroborate with the WAXS data of the thermosets, where a new signal, related to the flexible thioether structures was found.

The T_g for the hardwood lignin-based thermosets was higher than the corresponding softwood samples by 9–30 °C. The main structural difference between softwood and hardwood is the content of syringyl units. The C_5-position in hardwood lignin samples is occupied by a methoxy group, and as a result hardwood lignin is less condensed. The presence of methoxy groups also introduce mobility restrictions around the allyl aryl ether bonds due to steric hindrance. In previous studies, it was shown that hardwood lignin fractions have a higher content of the β-O-4' linkages compared to softwood lignin fractions.[80] The hardwood lignin samples have a slighty lower allyl content, resulting in a lower cross-link density. This results in a higher lignin content and less fewer flexible thioether bonds. The differences in T_g is a result of all above mentioned structural differences. The uniaxial tensile stress-stain data of T3-DAC-SW-Lignin samples showed an average Young's modulus (E) comprised between 1.4 and 2.3 GPa, a tensile stress at break (σ_b) comprised between 19 and 49 MPa, and an elongation at break (ε_b) comprised between 1.6 and 5.8%. These thermosets showed relatively good thermo-stability, with no degradation up to 200 °C.

Study B: Lignin thermosets from microwave-assisted extraction (Paper IV)

As previously described, the microwave-assisted extraction and functionalization present an efficient processing technique. The selected allylated sample, DAC-SW-IPA-120-I-s, can be compared to the allylated ethyl acetate softwood solvent extracted fraction, considering similarities in molecular weight and functionalities. The allylated sample was mixed with

the trifunctional cross-linker. The thiol-ene ratio was kept at 1:1. The composition of the thermosets is shown in Table 2. The curing performance of this sample was investigated by RT-FTIR (Figure 23). It was observed that for this resin formulation, the 95% thiol conversion was achieved after 19.5 h. The curing performance of this resin was faster in comparison with the previously studied thermosets from the sequential solvent fractionation of softwood lignin. This is well in line with the differences in the lignin composition as discussed when comparing softwood and hardwood base resins.

This could be related to the differences in the lignin chemical structure, molecular weight, distribution of the OH groups, the content of the unmodified OH groups, and the lignin morphology. Previously it was noticed that the softwood and hardwood lignin samples showed differences in the total phenolic OH content (especially guaiacyl OH groups) and the aliphatic OH content before chemical modification. For SW-IPA-120-I-s sample, the aliphatic OH groups content was higher compared to the SW-EtOAc fraction and the guaiacyl OH groups content was lower. Again, this emphasizes the importance of the distribution of the OH groups content in the retrieved fractions.

Thiol conversion (%)	**Curing time (h)**
20	2.2
50	7.5
75	13.2
95	19.5
100	21.1

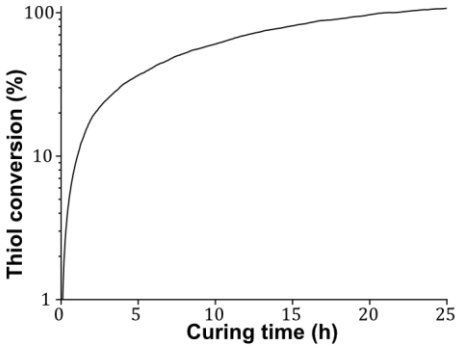

Figure 23. The thiol signal conversion (2607–2533 cm^{-1}) in function of time for T3-DAC-SW-IPA-120-I-s lignin resin formulation at 125 °C. Adapted from ref. 92.

The final thermoset properties were in line with those obtained from allylated softwood fractions obtained by solvent extraction, showing a T_g of 105 ± 3 °C (Figure 24). It can thus be concluded that microwave-assisted

processes represent an alternative route to obtain thiol-ene thermoset polymers in a benign way.

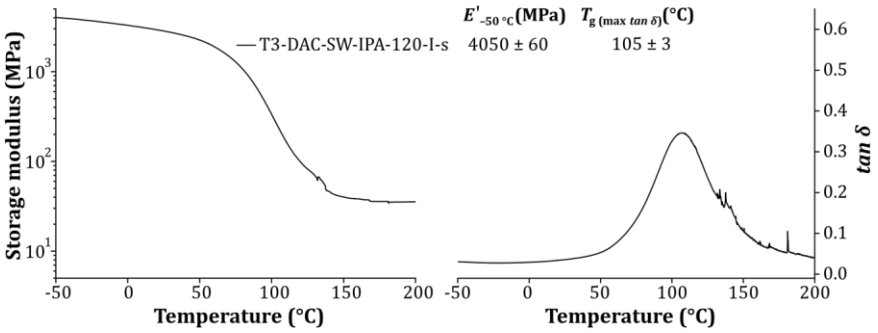

Figure 24. Representative DMA curves of the T3-DAC-SW-IPA-120-I-s lignin-based thermoset. Storage modulus (E') is illustrated on the left and *tan δ* signal on the right. Adapted from ref. 92.

5 Conclusions

In this thesis, different approaches of lignin fractionation, chemical modification, and thermal cross-linking were investigated. The main goal was to produce lignin-based thermosets with tunable mechanical and morphological properties and to understand their structure-properties relationships.

It was shown that using different lignin extraction procedures, such as solvent fractionation or microwave-extraction, it is possible to retrieve lignin fractions with tunable properties. By fractionating technical softwood or hardwood lignin, more homogeneous fractions can be retrieved. These fractions differ in terms of molecular weight, dispersity, distribution of the OH groups, and their nanoscale morphology.

The reactivity of the lignin samples was enhanced by chemically modifying the OH groups. The chemical modification enables the use of lignin samples as starting materials for resin synthesis. The incorporation of allyl groups was achieved in two ways: with allyl chloride and with diallyl carbonate. The allylation with allyl chloride is selective towards the phenolic OH groups, while diallyl carbonate reacts with all OH groups that are present. The obtained lignin samples had different content of the allyl functionalities and can be used as a constituent of thiol-ene thermosets.

The allylated lignins were thermally cured with different thiol cross-linkers through thiol-ene chemistry. The produced lignin-based thermosets displayed relatively high T_g's for a thiol-ene system. This was mainly related to the aromatic backbone structure of lignin, cross-link density, the polarity associated with the OH groups, and the noncovalent interactions, such as π-π stacking interactions.

It was possible to tune the mechanical properties of the thermosets using lignins from different sources (such as softwood or hardwood), performing different extraction procedures (solvent fractionation or microwave-extraction), or varying the thiol cross-linkers (their polyfunctionality).

The mechanical properties of the lignin-based thermosets can be varied by keeping the lignin fraction constant and changing the thiol cross-linking agent. The produced lignin-based thermosets showed variations in both, storage modulus and T_g. With an increasing number of thiol groups on the cross-linking agent, the T_g of the thermosets increased.

The mechanical properties of the lignin-based thermosets can also be varied using highly modified technical lignins from different sources. The high allyl content and low amount of polar groups, such as OH groups, result in lignin-based thermosets with properties dominated by the flexible thioether linkages.

It was also shown that using microwave-extracted lignin, it is possible to obtain lignin-based thermosets with relatively low T_g, where the properties are mainly influenced by the molecular weight of the lignin component, thioether content, and polarity of the system.

The obtained lignin-thermosets showed significant morphological differences at nanoscale. The presence of different repeating features, such as lignin superstructures or π–π interactions (sandwiched and T-shaped) was identified. These features varied in the different lignin fractions and the lignin-based thermosets, thus influencing their properties.

In conclusion, this work highlights the significant role of the morphological and mechanical characteristics of the produced lignin-based thermosets in determining their structure-property relationships.

6 Future work

In this thesis, the structure-property relationships of thiol-ene lignin-based thermosets were elucidated.

It will be interesting to investigate the possible applications of these thermosets as adhesives or as composite matrices where the main focus is on their mechanical performance and not appearance. Properties, such as permeability, solvent resistance, and degradation mechanism, need to be studied in order to understand the potential applications.

In terms of chemical modification, new routes can be explored. Allyl chloride can also be replaced with more sustainable and non-toxic reagents. The reaction conditions with diallyl carbonate can be further improved using lower loadings of the catalyst and lower temperatures. A more sustainable crosslinking reagent should be investigated, such as elemental sulfur. There is a need to produce fully bio-based, but also recyclable lignin-based thermosets.

A better understanding of lignin morphology at nanoscale will provide important insight for elucidating the structure of native lignin. In situ WAXS studies during the film formation will provide missing knowledge of the lignin superstructure formation. The exact effect of the π-π stacking interactions on the lignin properties needs to be understood and quantified. These characteristics will provide the missing information on how the noncovalent interactions, such as π-π stacking interactions and hydrogen bonding, influence the lignin aggregation and self-assembly.

In conclusion, there is room for improvements to be done in terms of environmental impact and sustainability of the produced thermosets.

7 Acknowledgements

I would like to acknowledge the Knut and Alice Wallenberg foundation for funding this Ph. D. project through the Wallenberg Wood Science Center.

I am deeply grateful to my supervisor, Prof. Mats Johansson, for providing me with the opportunity to carry out this research. Mats, your guidance and support throughout these four years has been truly invaluable. Thank you for always keeping your door open. Thank you for your patience with my English spelling. I often struggled with expressing my thoughts and ideas accurately. I am grateful for your dedication in this regard. Your expertise has played a crucial role in shaping me as a researcher and writer. Your mentorship extended beyond the boundaries of academia, as you constantly showed genuine interest in my well-being and development as an individual.

I would also like to express my gratitude to my co-supervisors, Prof. Martin Lawoko and Prof. Stephan Roth. Martin, your expertise and passion for lignin have been a constant source of inspiration for me. Stephan, thank you for all the support and availability.

Thank you, Mats, Martin, and Stephan for continuously sharing your knowledge and expertise. It was a pleasure to have the opportunity to pursue my PhD under your supervision.

I would like to thank all the seniors of the Coating division and WWSC for being so supportive. A special thanks goes to Dr. Daniel Hutchinson for continuously improving our lab. Thank you for accepting to be the chair at my defense. A big thanks goes to Assoc. Prof. Markus Kärkäs for reviewing this thesis.

I am grateful to my co-authors for their valuable contributions to the research and writing process; Prof. Stephan V. Roth, Prof. Michael A. R. Meier, Prof. Minna Hakkarainen, Docent Olena Sevastyanova, Dr. Marcus E. Jawerth, Dr. Calvin J. Brett, Dr. Benedikt Sochor, Dr. Andrei Chumakov, Dr. Matthias Schwartzkopf, Marie Betker, Alessio Truncali, Jenevieve Gocheco Yao. I look forward to the possibility of future collaborations with you.

The most precious aspect of my PhD are the relationships that has been formed with my colleagues and I am so happy to call you my friends.

Rosella Telaretti Leggieri, during these four years, you have been an integral part of my PhD journey. We shared every success and disappointment. We spent long nights in the lab, creating memories that will stay with us forever. We attended conferences together where crazy things

happened all the time (went to explore Sant Diego's beaches, spent an evening in Hollywood with the Oscar nominee, explored the Amsterdam by night, long shifts at DESY). During the pandemic we were inseparable (only me and you, in the middle of the sea, kayaking). Faridah Namata, you bring sunshine to every moment. Thank you for all the amazing moments during the WWSC schools (especially swimming with jelly fishes in the death cold weather), lab days (late night inventory), and after work activities (sorry for screaming so laud at the Sam Smith concert). You both made it so easy to go through all the difficult moments. The memories created together are priceless. I sincerely appreciate your friendship and I love you.

Marcus Jawerth, thank you for all your support and fun that we had together in the lab. A special thanks to Benedikt Sochor, Marie Betker, and Constantin Harder for the best beam-times one can ever imagine. The sleepless nights at DESY are unforgettable. Benedikt, I am so grateful for your help with synchrotron data processing and your willingness to fit the data multiple times. Thank you, Calvin Brett, for starting the synchrotron journey. Nicola Giummarella, thank you for always taking the time to stop and have "due chiacchiere". Anastasia Ryazanova, thanks for introducing me to the fascinating world of microscopy, as well as the joy of dancing. I thoroughly enjoyed our dance classes together and I sincerely hope that we can practice more in the future. Thank you for being such a nice friend.

A special thank you to Tijana Todorovic and Maryam Mousa who never said no to any of my requests. Thanks for coming with me to the cat cafe, visit alpacas, and enjoy the best lunch breaks at "Flying Fish". You are amazing. Thanks to all present and former colleagues at Coating division and WWSC for making it so easy and fun. Thank you, Olivia Wilson, for proof reading my thesis. Åsa, thanks for the positive energy you bring and for being such a supportive and helpful friend. WWSC schools and workshops were fantastic, because of you: Monika Tolgo, Maria Karlsson, Angelica Avella, Rohan Ajit Kulkarni, Farhiya Alex Sellman, Maria Cortes Ruiz, Ahmad Reza Motezakker, Natalia Fijol, Gabriella Mastantuoni, Linnea Cederholm, Korneliya Gordeyeva, and Celine Montanari. Thanks a lot.

Spending just two months in Germany did not stop me for making new friends, and I am so grateful for the wonderful people I met there, and in particular Michael Rhein, Jonas Wolfs, Bohn Philipp, Roman Nickisch, Anja Kirchberg, Clara Scheelje, Francesca Destaso. Miki thanks for organizing the Europa-Park trip and letting me to spend time with your amazing dogs. Jonas

and Bohni, thank you for accepting the challenge to come with me to Lofoten. Those days were fantastic. Jonas, thanks for making my dream come true, driving up north with me and see the northern lights.

There are not enough words to explain how much do I appreciate the endless love, patience, support, understanding, and encouragement of my family; mom Ludmila, Doamna Tatiana, matusa Galea, bunica Tatiana, Sergiu, si fratele Alexandru. Mamica multumesc pentru tot. Thanks to my childhood friends Cristina Spitca and Nicoleta Saculteanu who always supported me and have been a part of my life journey. I love you all/Va iubesc la infinit.

This work is dedicated to the memory of my beloved bunelu Vanea. The love of learning and appreciation of hard work comes from you. I will forever miss you and never forget. Even if you are not with us anymore, your love and kindness will continue to guide me throughout my life.

Lelo, thank you for all your love and support. Thank you for taking care of me and believing in me. I feel lucky to have a partner who is equally crazy and likes my craziness. You accept me as I am and make me feel safe. Thanks for making time and joining me on my 30th birthday trip. It was amazing shopping together, eat McDonalds food, and go to sauna (upps). It feels like I will stay in Sweden now :) I yunami you.

It is impossible to acknowledge everyone who contributed to this part of my life and deserves my appreciation, I want you all to know that none of you have been forgotten (yet)!

Iuliana Ribca
Stockholm, May 2023

References

1. *United Nations, The 17 Sustainable Development Goals*. https://sdgs.un.org/goals, **accesed on 30.04.2023**.
2. Brundtland, G H *Report of the World Commission on Environment and Development: Our Common Future*; **1987.**
3. Pandey, D; Agrawal, M; Pandey, J S, Carbon footprint: current methods of estimation. *Environmental Monitoring and Assessment* **2011,** *178* (1-4), 135-160.
4. Cabeza, L F; Barreneche, C; Miró, L; Morera, J M; Bartolí, E; Inés Fernández, A, Low carbon and low embodied energy materials in buildings: A review. *Renewable and Sustainable Energy Reviews* **2013,** *23*, 536-542.
5. Tardy, B L; Lizundia, E; Guizani, C; Hakkarainen, M; Sipponen, M H, Prospects for the integration of lignin materials into the circular economy. *Materials Today* **2023.**
6. Green, M L; Espinal, L; Traversa, E; Amis, E J, Materials for sustainable development. *MRS Bulletin* **2012,** *37* (4), 303-309.
7. Raj, A; Jhariya, M K; Yadav, D K; Banerjee, A, Forest for Resource Managment and Enviromental Protection. In *Enviromental and Sustainable Development Through Forestry and Other Resources*., Banerjee, A.; Jhariya, M. K.; Yadav, D. K.; Raj, A., Eds. Apple Academic Press Inc.: Canada, **2020**; p 387.
8. Raj, T; Chandrasekhar, K; Naresh Kumar, A; Kim, S-H, Lignocellulosic biomass as renewable feedstock for biodegradable and recyclable plastics production: A sustainable approach. *Renewable and Sustainable Energy Reviews* **2022,** *158.*
9. Bertella, S; Luterbacher, J S, Lignin Functionalization for the Production of Novel Materials. *Trends in Chemistry* **2020,** *2* (5), 440-453.
10. Crestini, C; Lange, H; Sette, M; Argyropoulos, D S, On the structure of softwood kraft lignin. *Green Chemistry* **2017,** *19* (17), 4104-4121.
11. Calvo-Flores, F G, Lignin: A Renewable Raw Material. In *Encyclopedia of Renewable and Sustainable Materials*, Hashmi, S.; Choudhury, I. A., Eds. Elsevier: **2020**; pp 102-118.
12. Ralph, J; Lundquist, K; Brunow, G; Lu, F; Kim, H; Schatz, P F; Marita, J M; Hatfield, R D; Ralph, S A; Christensen, J H; Boerjan, W, Lignins: Natural polymers from oxidative coupling of 4-hydroxyphenyl- propanoids. *Phytochemistry Reviews* **2004,** *3* (1-2), 29-60.
13. Gellerstedt, G; Henriksson, G, Lignins: Major Sources, Structure and Properties. In *Monomers, Polymers and Composites from Renewable Resource*, Belgacem, M. N.; Gandini, A., Eds. Elsevier: **2008**; pp 201-224.
14. Vanholme, R; Demedts, B; Morreel, K; Ralph, J; Boerjan, W, Lignin Biosynthesis and Structure. *Plant Physiology* **2010,** *153* (3), 895-905.
15. Fernández-Rodríguez, J; Erdocia, X; Hernández-Ramos, F; Alriols, M G; Labidi, J, Lignin Separation and Fractionation by Ultrafiltration. In

Separation of Functional Molecules in Food by Membrane Technology, Bandeira, N. R., Ed. Andre Gerhard Wolff Acquisition: **2019**; pp 229-265.
16. Fengel, D; Wegener, G, *Wood - Chemistry, Ultrastructure, Reactions*. Walter de Gruyter: New York, **1989**; p 618.
17. Nasrullah, A; Bhat, A H; Sada Khan, A; Ajab, H, Comprehensive approach on the structure, production, processing, and application of lignin. In *Lignocellulosic Fibre and Biomass-Based Composite Materials*, **2017**; pp 165-178.
18. Boerjan, W; Ralph, J; Baucher, M, Lignin biosynthesis. *Annual Review of Plant Biology* **2003,** *54*, 519-546.
19. Katahira, R; Elder, T J; Beckham, G T, Chapter 1. A Brief Introduction to Lignin Structure. In *Lignin Valorization: Emerging Approaches*, The Royal Society of Chemistry: United States, **2018**; pp 1-20.
20. Abu-Omar, M M; Barta, K; Beckham, G T; Luterbacher, J S; Ralph, J; Rinaldi, R; Román-Leshkov, Y; Samec, J S M; Sels, B F; Wang, F, Guidelines for performing lignin-first biorefining. *Energy & Environmental Science* **2021,** *14* (1), 262-292.
21. Higuchi, T, Lignin Biochemistry - Biosynthesis and Biodegradation. *Wood Science and Technology* **1990,** *24* (1), 23-63.
22. Li, C; Zhao, X; Wang, A; Huber, G W; Zhang, T, Catalytic Transformation of Lignin for the Production of Chemicals and Fuels. *Chemical Reviews* **2015,** *115* (21), 11559-11624.
23. Meng, X; Crestini, C; Ben, H; Hao, N; Pu, Y; Ragauskas, A J; Argyropoulos, D S, Determination of hydroxyl groups in biorefinery resources via quantitative (31)P NMR spectroscopy. *Nature Protocols* **2019,** *14* (9), 2627-2647.
24. Balakshin, M; Capanema, E, On the Quantification of Lignin Hydroxyl Groups With 31P and 13C NMR Spectroscopy. *Journal of Wood Chemistry and Technology* **2015,** *35* (3), 220-237.
25. Cheng, K, Lignin characterization. In *Natural Polyphenols from Wood*, Elsevier Inc.: **2021**; pp 147-182.
26. El Mansouri, N-E; Salvadó, J, Analytical methods for determining functional groups in various technical lignins. *Industrial Crops and Products* **2007,** *26* (2), 116-124.
27. Huang, Y; Wang, L; Chao, Y; Nawawi, D S; Akiyama, T; Yokoyama, T; Matsumoto, Y, Analysis of Lignin Aromatic Structure in Wood Based on the IR Spectrum. *Journal of Wood Chemistry and Technology* **2012,** *32* (4), 294-303.
28. Terashima, N; Yoshida, M; Hafren, J; Fukushima, K; Westermark, U, Proposed supramolecular structure of lignin in softwood tracheid compound middle lamella regions. *Holzforschung* **2012,** *66* (8), 907-915.
29. Zhao, X; Huang, C; Xiao, D; Wang, P; Luo, X; Liu, W; Liu, S; Li, J; Li, S; Chen, Z, Melanin-Inspired Design: Preparing Sustainable Photothermal

Materials from Lignin for Energy Generation. *ACS Applied Materials & Interfaces* **2021,** *13* (6), 7600-7607.
30. Zhao, W; Xiao, L-P; Song, G; Sun, R-C; He, L; Singh, S; Simmons, B A; Cheng, G, From lignin subunits to aggregates: insights into lignin solubilization. *Green Chemistry* **2017,** *19* (14), 3272-3281.
31. Fabbri, F; Bischof, S; Mayr, S; Gritsch, S; Jimenez Bartolome, M; Schwaiger, N; Guebitz, G M; Weiss, R, The Biomodified Lignin Platform: A Review. *Polymers (Basel)* **2023,** *15* (7).
32. Mathew, A K; Abraham, A; Mallapureddy, K K; Sukumaran, R K, Lignocellulosic Biorefinery Wastes, or Resources? In *Waste Biorefinery*, Thallada Bhaskar; Ashok Pandey; S. Venkata Mohan; Duu-Jong Lee; Khanal, S. K., Eds. Elsevier: **2018**; pp 267-297.
33. Luo, H; Abu-Omar, M M, Chemicals From Lignin. In *Encyclopedia of Sustainable Technologies*, Abraham, M. A., Ed. Elsevier: **2017**; pp 573-585.
34. Kienberger, M; Maitz, S; Pichler, T; Demmelmayer, P, Systematic Review on Isolation Processes for Technical Lignin. *Processes* **2021,** *9* (5).
35. Tomani, P, The Lignoboost Process. *Cellulose Chemistry and Technology* **2010,** *44* (1-3), 53-58.
36. Lawoko, M; Samec, J S M, Kraft lignin valorization: Biofuels and thermoset materials in focus. *Current Opinion in Green and Sustainable Chemistry* **2023,** *40*.
37. Giummarella, N; Lindén, P A; Areskogh, D; Lawoko, M, Fractional Profiling of Kraft Lignin Structure: Unravelling Insights on Lignin Reaction Mechanisms. *ACS Sustainable Chemistry & Engineering* **2019,** *8* (2), 1112-1120.
38. Gigli, M; Crestini, C, Fractionation of industrial lignins: opportunities and challenges. *Green Chemistry* **2020,** *22* (15), 4722-4746.
39. Pang, T; Wang, G; Sun, H; Sui, W; Si, C, Lignin fractionation: Effective strategy to reduce molecule weight dependent heterogeneity for upgraded lignin valorization. *Industrial Crops and Products* **2021,** *165*.
40. Sadeghifar, H; Ragauskas, A, Perspective on Technical Lignin Fractionation. *ACS Sustainable Chemistry & Engineering* **2020,** *8* (22), 8086-8101.
41. Aminzadeh, S; Lauberts, M; Dobele, G; Ponomarenko, J; Mattsson, T; Lindström, M E; Sevastyanova, O, Membrane filtration of kraft lignin: Structural charactristics and antioxidant activity of the low-molecular-weight fraction. *Industrial Crops and Products* **2018,** *112*, 200-209.
42. Li, H; McDonald, A G, Fractionation and characterization of industrial lignins. *Industrial Crops and Products* **2014,** *62*, 67-76.
43. Ebrahimi Majdar, R; Ghasemian, A; Resalati, H; Saraeian, A; Crestini, C; Lange, H, Case Study in Kraft Lignin Fractionation: "Structurally Purified" Lignin Fractions—The Role of Solvent H-Bonding Affinity. *ACS Sustainable Chemistry & Engineering* **2020,** *8* (45), 16803-16813.

44. Passoni, V; Scarica, C; Levi, M; Turri, S; Griffini, G, Fractionation of Industrial Softwood Kraft Lignin: Solvent Selection as a Tool for Tailored Material Properties. *ACS Sustainable Chemistry & Engineering* **2016,** *4* (4), 2232-2242.
45. Duval, A; Vilaplana, F; Crestini, C; Lawoko, M, Solvent screening for the fractionation of industrial kraft lignin. *Holzforschung* **2016,** *70* (1), 11-20.
46. Park, S Y; Kim, J Y; Youn, H J; Choi, J W, Fractionation of lignin macromolecules by sequential organic solvents systems and their characterization for further valuable applications. *International Journal of Biological Macromolecules* **2018,** *106*, 793-802.
47. Gouveia, S; Fernandez-Costas, C; Sanroman, M A; Moldes, D, Enzymatic polymerisation and effect of fractionation of dissolved lignin from Eucalyptus globulus Kraft liquor. *Bioresource Technology* **2012,** *121*, 131-138.
48. Lourençon, T V; Hansel, F A; da Silva, T A; Ramos, L P; de Muniz, G I B; Magalhães, W L E, Hardwood and softwood kraft lignins fractionation by simple sequential acid precipitation. *Separation and Purification Technology* **2015,** *154*, 82-88.
49. Cui, C; Sun, R; Argyropoulos, D S, Fractional Precipitation of Softwood Kraft Lignin: Isolation of Narrow Fractions Common to a Variety of Lignins. *ACS Sustainable Chemistry & Engineering* **2014,** *2* (4), 959-968.
50. Dong, C; Feng, C; Liu, Q; Shen, D; Xiao, R, Mechanism on microwave-assisted acidic solvolysis of black-liquor lignin. *Bioresource Technology* **2014,** *162*, 136-141.
51. Cederholm, L; Xu, Y; Tagami, A; Sevastyanova, O; Odelius, K; Hakkarainen, M, Microwave processing of lignin in green solvents: A high-yield process to narrow-dispersity oligomers. *Industrial Crops and Products* **2020,** *145*.
52. Merino, O; Cerón-Camacho, R; Luque, R; Martínez-Palou, R, Microwave-Assisted Lignin Solubilization in Protic Ionic Compounds Containing 2,3,4,5-Tetraphenyl-1H-imidazolium and Inorganic Anions. *Waste and Biomass Valorization* **2019,** *11* (12), 6585-6593.
53. Sun, Y-C; Liu, X-N; Wang, T-T; Xue, B-L; Sun, R-C, Green Process for Extraction of Lignin by the Microwave-Assisted Ionic Liquid Approach: Toward Biomass Biorefinery and Lignin Characterization. *ACS Sustainable Chemistry & Engineering* **2019,** *7* (15), 13062-13072.
54. Figueiredo, P; Lintinen, K; Hirvonen, J T; Kostiainen, M A; Santos, H A, Properties and chemical modifications of lignin: Towards lignin-based nanomaterials for biomedical applications. *Progress in Materials Science* **2018,** *93*, 233-269.
55. Stark, K; Taccardi, N; Bosmann, A; Wasserscheid, P, Oxidative depolymerization of lignin in ionic liquids. *ChemSusChem* **2010,** *3* (6), 719-723.

56. Wang, M; Liu, M; Li, H; Zhao, Z; Zhang, X; Wang, F, Dealkylation of Lignin to Phenol via Oxidation–Hydrogenation Strategy. *ACS Catalysis* **2018,** *8* (8), 6837-6843.
57. Luo, K H; Zhao, S J; Fan, G Z; Cheng, Q P; Chai, B; Song, G S, Oxidative conversion of lignin isolated from wheat straw into aromatic compound catalyzed by NaOH/NaAlO(2). *Food Science and Nutrition* **2020,** *8* (7), 3504-3514.
58. Fache, M; Boutevin, B; Caillol, S, Vanillin Production from Lignin and Its Use as a Renewable Chemical. *ACS Sustainable Chemistry & Engineering* **2015,** *4* (1), 35-46.
59. Liu, L-Y; Hua, Q; Renneckar, S, A simple route to synthesize esterified lignin derivatives. *Green Chemistry* **2019,** *21* (13), 3682-3692.
60. Duval, A; Avérous, L, Cyclic Carbonates as Safe and Versatile Etherifying Reagents for the Functionalization of Lignins and Tannins. *ACS Sustainable Chemistry & Engineering* **2017,** *5* (8), 7334-7343.
61. Jiang, X; Liu, J; Du, X; Hu, Z; Chang, H-m; Jameel, H, Phenolation to Improve Lignin Reactivity toward Thermosets Application. *ACS Sustainable Chemistry & Engineering* **2018,** *6* (4), 5504-5512.
62. Moreno, A; Liu, J; Morsali, M; Sipponen, M H, Chemical modification and functionalization of lignin nanoparticles. In *Micro and Nanolignin in Aqueous Dispersions and Polymers*, Debora Puglia, C. S., Fabrizio Sarasini, Ed. Elsevier: **2022**; pp 385-431.
63. Laurichesse, S; Avérous, L, Chemical modification of lignins: Towards biobased polymers. *Progress in Polymer Science* **2014,** *39* (7), 1266-1290.
64. Jawerth, M; Johansson, M; Lundmark, S; Gioia, C; Lawoko, M, Renewable Thiol-Ene Thermosets Based on Refined and Selectively Allylated Industrial Lignin. *ACS Sustainable Chemistry & Engineering* **2017,** *5* (11), 10918-10925.
65. Zoia, L; Salanti, A; Frigerio, P; Orlandi, M, Exploring Allylation and Claisen Rearrangement as a Novel Chemical Modification of Lignin. *BioResources* **2014,** *9*, 6540-6561.
66. Over, L C; Meier, M A R, Sustainable Allylation of Organosolv Lignin with Diallyl Carbonate and detailed Structural Characterization of modified Lignin. *Green Chemistry* **2016,** *18* (1), 197-207.
67. Liu, X; Wang, J; Yu, J; Zhang, M; Wang, C; Xu, Y; Chu, F, Preparation and characterization of lignin based macromonomer and its copolymers with butyl methacrylate. *International Journal of Biological Macromolecules* **2013,** *60*, 309-315.
68. Gordobil, O; Moriana, R; Zhang, L; Labidi, J; Sevastyanova, O, Assesment of technical lignins for uses in biofuels and biomaterials: Structure-related properties, proximate analysis and chemical modification. *Industrial Crops and Products* **2016,** *83*, 155-165.

69. Margarita, C; Di Francesco, D; Tuñon, H; Kumaniaev, I; Rada, C J; Lundberg, H, Mild and selective etherification of wheat straw lignin and lignin model alcohols by moisture-tolerant zirconium catalysis. *Green Chemistry* **2023,** *25* (6), 2401-2408.
70. Duval, A; Averous, L, Solvent- and Halogen-Free Modification of Biobased Polyphenols to Introduce Vinyl Groups: Versatile Aromatic Building Blocks for Polymer Synthesis. *ChemSusChem* **2017,** *10* (8), 1813-1822.
71. Hua, Q; Liu, L Y; Cho, M; Karaaslan, M A; Zhang, H; Kim, C S; Renneckar, S, Functional Lignin Building Blocks: Reactive Vinyl Esters with Acrylic Acid. *Biomacromolecules* **2023,** *24* (2), 592-603.
72. Jawerth, M E; Brett, C J; Terrier, C; Larsson, P T; Lawoko, M; Roth, S V; Lundmark, S; Johansson, M, Mechanical and Morphological Properties of Lignin-Based Thermosets. *ACS Applied Polymer Materials* **2020,** *2*, 668-676.
73. AlMaadeed, M A A; Ponnamma, D; El-Samak, A A, Polymers to improve the world and lifestyle: physical, mechanical, and chemical needs. In *Polymer Science and Innovative Applications*, AlMaadeed, M. A. A.; Ponnamma, D.; Carignano, M. A., Eds. **2020**; pp 1-19.
74. Liu, J; Zhang, L; Shun, W; Dai, J; Peng, Y; Liu, X, Recent development on bio-based thermosetting resins. *Journal of Polymer Science* **2021,** *59* (14), 1474-1490.
75. Ratna, D, Chemitry and general applications of thermoset resins. In *Recent advances and applications of thermoset resins*, Payne, E., Ed. Elsevier: Chennai, India, **2022**; Vol. Second Edition, p 583.
76. Dotan, A, Biobased Thermosets. In *Handbook of Thermoset Plastics*, **2014**; pp 577-622.
77. Wang, Y-Y; Wyman, C E; Cai, C M; Ragauskas, A J, Lignin-Based Polyurethanes from Unmodified Kraft Lignin Fractionated by Sequential Precipitation. *ACS Applied Polymer Materials* **2019,** *1* (7), 1672-1679.
78. Nikafshar, S; Wang, J; Dunne, K; Sangthonganotai, P; Nejad, M, Choosing the Right Lignin to Fully Replace Bisphenol A in Epoxy Resin Formulation. *ChemSusChem* **2021,** *14* (4), 1184-1195.
79. Gioia, C; Lo Re, G; Lawoko, M; Berglund, L, Tunable Thermosetting Epoxies Based on Fractionated and Well-Characterized Lignins. *Journal of the American Chemical Society* **2018,** *140* (11), 4054-4061.
80. Gioia, C; Colonna, M; Tagami, A; Medina, L; Sevastyanova, O; Berglund, L A; Lawoko, M, Lignin-Based Epoxy Resins: Unravelling the Relationship between Structure and Material Properties. *Biomacromolecules* **2020,** *21* (5), 1920-1928.
81. Moreno, A; Morsali, M; Sipponen, M H, Catalyst-Free Synthesis of Lignin Vitrimers with Tunable Mechanical Properties: Circular Polymers and Recoverable Adhesives. *ACS Applied Materials and Interfaces* **2021,** *13* (48), 57952-57961.

82. Zhang, S; Liu, T; Hao, C; Wang, L; Han, J; Liu, H; Zhang, J, Preparation of a lignin-based vitrimer material and its potential use for recoverable adhesives. *Green Chemistry* **2018,** *20* (13), 2995-3000.
83. Hao, C; Liu, T; Zhang, S; Brown, L; Li, R; Xin, J; Zhong, T; Jiang, L; Zhang, J, A High-Lignin-Content, Removable, and Glycol-Assisted Repairable Coating Based on Dynamic Covalent Bonds. *ChemSusChem* **2019,** *12* (5), 1049-1058.
84. Zhang, W; Wang, B; Xu, X; Feng, H; Hu, K; Su, Y; Zhou, S; Zhu, J; Weng, G; Ma, S, Green and facile method for valorization of lignin to high-performance degradable thermosets. *Green Chemistry* **2022,** *24* (24), 9659-9667.
85. Buono, P; Duval, A; Averous, L; Habibi, Y, Lignin-Based Materials Through Thiol-Maleimide "Click" Polymerization. *ChemSusChem* **2017,** *10* (5), 984-992.
86. Braun, J v; Murjahn, R, Haftfestigkeit organischer Reste (IV). *Berichte der Deutschen Chemischen Gesellschaft (A and B series)* **1926,** *59* (6), 1202-1209.
87. Lowe, A B, Thiol-ene “click” reactions and recent applications in polymer and materials synthesis. *Polymer Chemistry* **2010,** *1* (1), 17-36.
88. Hoyle, C E; Bowman, C N, Thiol-Ene Click Chemistry. *Angewandte Chemie International Edition* **2010,** *49* (9), 1540-1573.
89. Chan, J W; Hoyle, C E; Lowe, A B; Bowman, M, Nucleophile-Initiated Thiol-Michael Reactions: Effect of Organocatalyst, Thiol, and Ene. *Macromolecules* **2010,** *43* (15), 6381-6388.
90. Hoyle, C E; Lee, T Y; Roper, T, Thiol-enes: Chemistry of the past with promise for the future. *Journal of Polymer Science Part A: Polymer Chemistry* **2004,** *42* (21), 5301-5338
91. Ribca, I; Jawerth, M E; Brett, C J; Lawoko, M; Schwartzkopf, M; Chumakov, A; Roth, S V; Johansson, M, Exploring the Effects of Different Cross-Linkers on Lignin-Based Thermoset Properties and Morphologies. *ACS Sustainable Chemistry & Engineering* **2021,** *9* (4), 1692-1702.
92. Truncali, A; Ribca, I; Yao, J G; Hakkarainen, M; Johansson, M. (2023). Microwave-assisted fractionation and functionalization of technical lignin towards thermoset resins [Manuscript].
93. Jawerth, M; Lawoko, M; Lundmark, S; Perez-Berumen, C; Johansson, M, Allylation of a lignin model phenol: a highly selective reaction under benign conditions towards a new thermoset resin platform. *RSC Advances* **2016,** *6* (98), 96281-96288.
94. Over, L C. Sustainable Derivatization of Lignin and Subsequent Synthesis of Cross-Linked Polymers. Karlsruhe Institute of Technology (KIT), **2017**.
95. Ribca, I; Sochor, B; Roth, S V; Lawoko, M; Meier, M A R; Johansson, M. (2023). Effect of molecular organization on the properties of fractionated

lignin-based thiol-ene thermoset materials [Manuscript submitted for publication].
96. Ribca, I; Sochor, B; Betker, M; Roth, S V; Lawoko, M; Sevastyanova, O; Meier, M A R; Johansson, M, Impact of lignin source on the performance of thermoset resins. *Europen Polymer Journal* **2023**, 194, 112141.
97. Chiou, B-S; Khan, S A, Real-Time FTIR and in Situ Rheological Studies on the UV Curing Kinetics of Thiol-ene Polymers. *Macromolecules* **1997,** (30), 7322-7328.
98. Sadeghifar, H; Wells, T; Le, R K; Sadeghifar, F; Yuan, J S; Jonas Ragauskas, A, Fractionation of Organosolv Lignin Using Acetone:Water and Properties of the Obtained Fractions. *ACS Sustainable Chemistry & Engineering* **2016,** *5* (1), 580-587.
99. Zhao, X B; Liu, D H, Chemical and thermal characteristics of lignins isolated from Siam weed stem by acetic acid and formic acid delignification. *Industrial Crops and Products* **2010,** *32* (3), 284-291.
100. Rinaldi, R; Jastrzebski, R; Clough, M T; Ralph, J; Kennema, M; Bruijnincx, P C; Weckhuysen, B M, Paving the Way for Lignin Valorisation: Recent Advances in Bioengineering, Biorefining and Catalysis. *Angewandte Chemie International Edition* **2016,** *55* (29), 8164-215.
101. Hunter, C A; Sanders, J K M, The Nature of π-π Interactions. *Journal of the American Chemical Society* **1990,** *112* (14), 5524-5534.
102. Sinnokrot, M O; Valeev, E F; Sherrill, C D, Estimates of the ab initio limit for pi-pi interactions: the benzene dimer. *Journal of the American Chemical Society* **2002,** *124* (36), 10887-10893.
103. Chen, T; Li, M; Liu, J, π–π Stacking Interaction: A Nondestructive and Facile Means in Material Engineering for Bioapplications. *Crystal Growth & Design* **2018,** *18* (5), 2765-2783
104. Wang, Y Y; Chen, Y R; Sarkanen, S, Blend configuration in functional polymeric materials with a high lignin content. *Faraday Discussions* **2017,** *202*, 43-59.
105. Chen, Y R; Sarkanen, S; Wang, Y Y, Lignin-Only Polymeric Materials Based on Unmethylated Unfractionated Kraft and Ball-Milled Lignins Surpass Polyethylene and Polystyrene in Tensile Strength. *Molecules* **2019,** *24* (24).
106. Gedye, R; Smith, F; Westaway, K; Ali, H; Baldisera, L; Laberge, L; Rousell, J, The Use of Microwave-Ovens for Rapid Organic-Synthesis. *Tetrahedron Letters* **1986,** *27* (3), 279-282.
107. Liu, Q; Li, P; Liu, N; Shen, D, Lignin depolymerization to aromatic monomers and oligomers in isopropanol assisted by microwave heating. *Polymer Degradation and Stability* **2017,** *135*, 54-60.
108. Chollet, B; Lopez-Cuesta, J M; Laoutid, F; Ferry, L, Lignin Nanoparticles as A Promising Way for Enhancing Lignin Flame Retardant Effect in Polylactide. *Materials (Basel)* **2019,** *12* (13).

109. Monteil-Rivera, F; Paquet, L, Solvent-free catalyst-free microwave-assisted acylation of lignin. *Industrial Crops and Products* **2015,** *65*, 446-453
110. Yao, J; Odelius, K; Hakkarainen, M, Microwave Hydrophobized Lignin with Antioxidant Activity for Fused Filament Fabrication. *ACS Applied Polymer Materials* **2021,** *3* (7), 3538-3548.
111. Li, C L; Johansson, M; Sablong, R J; Koning, C E, High performance thiol-ene thermosets based on fully bio-based poly(limonene carbonate)s. *European Polymer Journal* **2017,** *96*, 337-349.
112. Bowman, C N; Kloxin, C J, Toward an enhanced understanding and implementation of photopolymerization reactions. *AIChE Journal* **2008,** *54* (11), 2775-2795.
113. Guerra, A; Gaspar, A R; Contreras, S; Lucia, L A; Crestini, C; Argyropoulos, D S, On the propensity of lignin to associate: a size exclusion chromatography study with lignin derivatives isolated from different plant species. *Phytochemistry* **2007,** *68* (20), 2570-2583.
114. Claudino, M; Mathevet, J-M; Jonsson, M; Johansson, M, Bringingd-limonene to the scene of bio-based thermoset coatings via free-radical thiol–ene chemistry: macromonomer synthesis, UV-curing and thermo-mechanical characterization. *Polymer Chemistry* **2014,** *5* (9), 3245-3260.